Electronic Supplementary Material (ESI) for ChemComm.
This journal is © The Royal Society of Chemistry 2019

Supporting Information for

Efficient Green Light-Excited Switches Based on Dithienylethenes with BF_2-doped π-Conjugated Systems

Ziyong Li,*[a] Yijie Dai,[a] Zhiqiang Lu,*[b] Yingying Pei,[a] Hong Chen,[a] Lilei Zhang,[b] Ying Duan,[a] Hui Guo*[b]

[a] Luoyang Key Laboratory of Organic Functional Molecules, School of Food and Drug, Luoyang Normal University, Luoyang, 471934, China

[b] College of Chemistry and Chemical Engineering, and Henan Key Laboratory of Function-Oriented Porous Materials, Luoyang Normal University, Luoyang, 471934, China

Corresponding author E-mail: liziyong@mails.ccnu.edu.cn; zqlu2000@163.com; guohui0319@nankai.edu.cn.

Table of Contents

1. General information

1.1 Materials

All manipulations are carried out under a nitrogen atmosphere by using standard Schlenk techniques unless otherwise stated. Tetrahydrofuran / toluene are distilled under nitrogen from sodium-benzophenone. The intermediates **4a**[1] and **4b**[2] are prepared by reported literature methods. MCF 7 cell lines are supplied by KeyGen Biotech. Co., Ltd. (China). All other starting materials are obtained commercially as analytical-grade from Energy Chemical Reagent Co., Ltd (Shanghai, China) and used without further purification. The relative quantum yields are determined by comparing the reaction yield with the known yield of 2-bis (2-methyl-5 -phenyl-3-thienyl) perfluorocyclopentene.[3]

1.2 Instruments

^{1}H and ^{13}C NMR spectra are collected on German BRUKER AVANCE III 400 MHz (all the chemical shifts are relative to TMS). High resolution mass spectra are obtained on SCIEX X-500R QTOF (ESI mode). All the absorption spectra are collected on a SHIMADZU UV-2600 UV-Vis spectrophotometer, and the fluorescence spectra are obtained on a Hitachi Model F-4500 fluorescent spectrophotometer. In the photochromic experiments, the visible light irradiation experiment is carried out using a 30 W green lamp (520 - 530 nm), 30 W red lamp (650 - 660 nm) and 30 W near-infrared lamp (800 - 810 nm), respectively. The confocal imaging experiments were subjected with TCS SP8 confocal laser scanning microscope (CLSM) (Leica, Germany).

1.3 Preparation of the PMMA film

The PMMA films are prepared by dissolving **1a-1d** (5.0 mg) and PMMA (100 mg) in $CHCl_3$ (2 mL), then the uniform solution is coated on the quartz plate (1.0 × 3.0 cm). The PMMA films are dried in air and stored in darkness.

1.4 Cell culture and confocal imaging

The cell experiments are performed as follows: MCF 7 cell lines are seeded in a glass-bottom dish with a density of ca. 5×10^4 cells per dish and incubated in medium of 1640 containing 10% fetal bovine serum (FBS) and 1% antibiotics (100 U mL^{-1} penicillin and 100 μg mL^{-1} streptomycin) at 37 °C in an atmosphere of 5% CO_2 in air for 24 h. After then, 10 μL solution of sample molecules

1a and **1b** in DMSO (1.0 mM) is slowly added to the dish containing the cells and 1.0 mL fresh culture medium. The culture medium is gently agitated along the inner wall of the dish with a pipette to make sample molecules disperse uniformly. Then the cells are incubated for 30 min at ambient temperature. Finally the cells are washed 3 times with PBS (pH = 7.4) to fully remove the uninternalized dyes. The confocal fluorescence microscopy is employed for the data collection. Fluorescence signals are collected at 530 - 750 nm upon excitation at 510 nm. The switchable irradiation experiments are conducted on green light at 520 - 530 nm and red light at 650 - 660 nm for 2 min respectively.

2. Experimental section

2.1 Scheme S1. Synthesis route of dithienylethenes **1a-1d**.

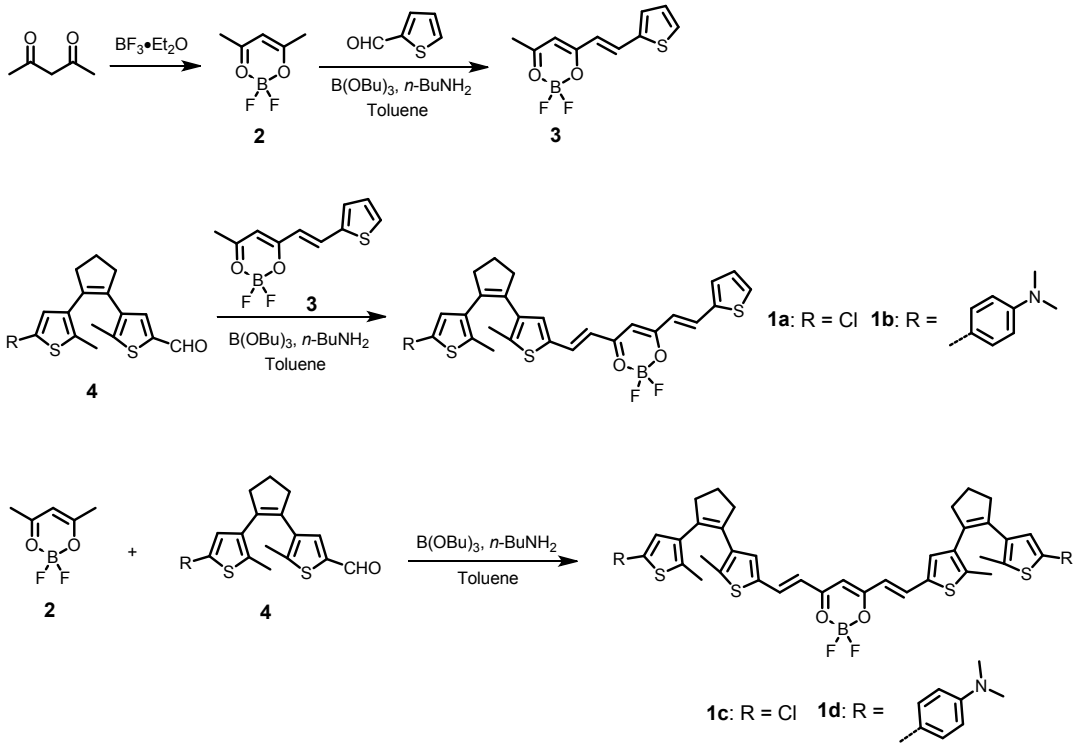

2.2 Synthesis and characterization

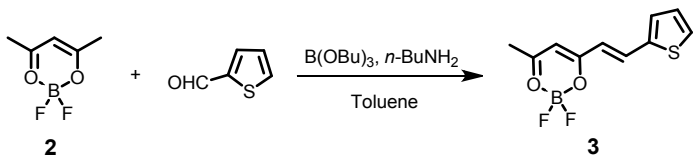

The solution of pentane-2, 4-dione (200 mg, 2.0 mmol) and $BF_3 \cdot OEt_2$ (0.26 mL, 2.0 mmol, 47%) in toluene (5 mL) is stirred at 65 °C for 2 h. Then the solution of thiophene-2-carbaldehyde (224

mg, 2.0 mmol) in toluene (2 mL) is added into the above reaction mixture, followed by $B(OBu)_3$ (0.81 mL, 3.0 mmol). The resulting solution is stirred for 30 min and *n*-butylamine (50 μL, 0.5 mmol) is slowly added, and stirred at 65 °C for 24 h. After cooling to room temperature, upon removel of solvent under reduced pressure and purified by column chromatography (silica gel: 200-300, PE : DCM = 1 : 1) to obtain the intermediate **3** as an orange solid (Yield: 56 %). ^{1}H NMR (400 MHz, $CDCl_3$) δ 8.19 (d, *J* = 15.2 Hz, 1H), 7.57 (d, *J* = 5.0 Hz, 1H), 7.44 (d, *J* = 3.6 Hz, 1H), 7.16 - 7.14 (m, 1H), 6.41 (d, *J* = 15.2 Hz, 1H), 5.96 (s, 1H), 2.33 (s, 3H). ^{13}C NMR (100 MHz, $CDCl_3$) δ 191.23, 180.32, 140.82, 139.65, 134.52, 132.10, 129.19, 118.53, 101.45, 24.49. HRMS (ESI-TOF) m/z: $[M + Na]^+$ Calcd for $C_{10}H_9BF_2NaO_2S$ 265.0282; Found 265.0285.

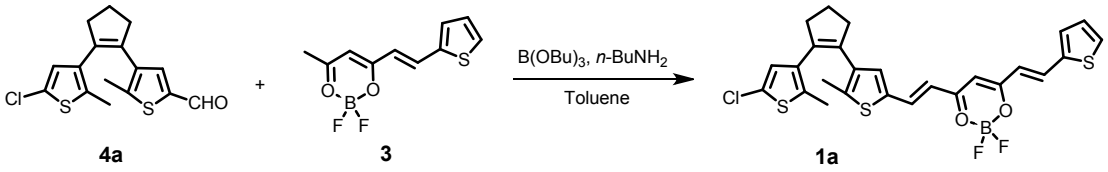

4a **3** **1a**

To a solution of intermediate **4a** (323 mg, 1.0 mmol) and **3** (242 mg, 1.0 mmol) in toluene (3 mL) is added $B(OBu)_3$ (0.41 mL, 1.5 mmol) and *n*-butylamine (25 μL, 0.25 mmol), and the resulting solution is stirred at 65 °C for 24 h. After cooling to room temperature, the solution is concentrated under reduced pressure and the residue is purified by column chromatography (silica gel: 200-300, PE : DCM = 1 : 2) to obtain the target compound **1a** as a brown solid (Yield: 61 %). ^{1}H NMR (400 MHz, $CDCl_3$) δ 8.12 (d, *J* = 15.2 Hz, 1H), 8.01 (d, *J* = 15.2 Hz, 1H), 7.53 (d, *J* = 4.5 Hz, 1H), 7.40 (d, *J* = 4.5 Hz, 1H), 7.14 - 7.12 (m, 1H), 7.10 (s, 1H), 6.58 (s, 1H), 6.47 (d, *J* = 15.2 Hz, 1H), 6.29 (d, *J* = 15.2 Hz, 1H), 5.95 (s, 1H), 2.79 - 2.73 (m, 4H), 2.10 - 2.06 (m, 2H), 2.05 (s, 3H), 1.85 (s, 3H). ^{13}C NMR (100 MHz, $CDCl_3$) δ 179.27, 178.43, 143.43, 139.93, 139.73, 138.86, 138.18, 136.03, 135.93, 135.56, 134.57, 133.82, 133.63, 133.33, 131.27, 128.89, 126.53, 125.61, 119.46, 117.93, 101.82, 38.38, 38.27, 22.82, 15.23, 14.10. HRMS (ESI-TOF) m/z: $[M + H]^+$ Calcd for $C_{26}H_{23}BClF_2O_2S_3$ 547.0610; Found 547.0612; $[M + Na]^+$ Calcd for $C_{26}H_{22}BClF_2NaO_2S_3$ 569.0429; Found 569.0445.

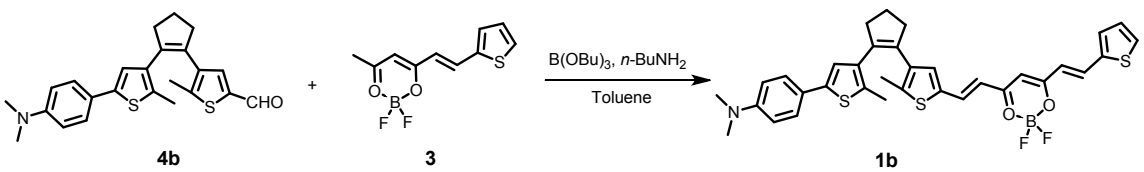

4b **3** **1b**

To a solution of intermediate **4b** (407 mg, 1.0 mmol) and **3** (242 mg, 1.0 mmol) in toluene (3 mL) is added $B(OBu)_3$ (0.41 mL, 1.5 mmol) and *n*-butylamine (25 μL, 0.25 mmol), and the resulting solution is stirred at 65 °C for 48 h. After cooling to room temperature, the solution is concentrated under reduced pressure and the residue is purified by column chromatography (silica gel: 200-300, PE : DCM = 1 : 4) to obtain the target compound **1b** as a brown solid (Yield: 48 %). ^{1}H NMR (400 MHz, $CDCl_3$) δ 8.13 (d, *J* = 15.2 Hz, 1H), 8.05 (d, *J* = 15.1 Hz, 1H), 7.54 (d, *J* = 4.6 Hz, 1H), 7.39 (d, *J* = 8.9 Hz, 3H), 7.19 (s, 1H), 7.15 - 7.13 (m, 1H), 6.82 (s, 1H), 6.73 (d, *J* = 8.5 Hz, 2H), 6.48 (d, *J* = 15.2 Hz, 1H), 6.30 (d, *J* = 15.1 Hz, 1H), 5.96 (s, 1H), 2.99 (s, 6H), 2.86 - 2.80 (m, 4H), 2.15 - 2.09 (m, 2H), 2.06 (s, 3H), 1.97 (s, 3H). ^{13}C NMR (100 MHz, $CDCl_3$) δ 179.52, 178.31, 149.99, 144.04, 141.16, 140.13, 138.87, 138.77, 137.01, 136.33, 135.96, 133.66, 132.81, 132.40, 131.31, 129.02, 126.43, 123.02, 121.49, 119.69, 117.83, 112.75, 101.93, 40.65, 38.63, 38.45, 23.09, 15.44, 14.41. HRMS (ESI-TOF) m/z: $[M + H]^+$ Calcd for $C_{34}H_{33}BF_2NO_2S_3$ 632.1735; Found 632.1725.

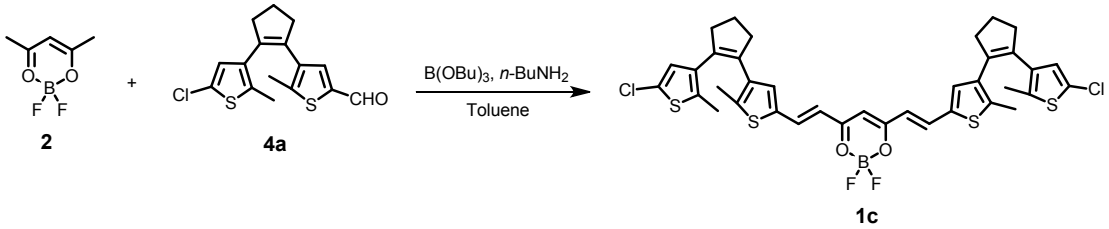

The solution of pentane-2, 4-dione (100 mg, 1.0 mmol) and $BF_3{\cdot}OEt_2$ (0.13 mL, 1.0 mmol, 47%) in toluene (3 mL) is stirred at 65 °C for 2 h. Then the solution of intermediate **4a** (646 mg, 2.0 mmol) in toluene (3 mL) is added into the above reaction mixture, followed by $B(OBu)_3$ (0.81 mL, 3.0 mmol). The resulting solution is stirred for 30 min and *n*-butylamine (50 μL, 0.5 mmol) is slowly added, and stirred at 65 °C for 24 h. After cooling to room temperature, the solution is concentrated under reduced pressure and the residue is purified by column chromatography (silica gel: 200-300, PE : DCM = 1 : 2) to obtain the target compound **1c** as a brown solid (Yield: 55 %). ^{1}H NMR (400 MHz, $CDCl_3$) δ 7.98 (d, *J* = 15.0 Hz, 2H), 7.08 (s, 2H), 6.58 (s, 2H), 6.27 (d, *J* = 15.0 Hz, 2H), 5.90 (s, 1H), 2.78 - 2.73 (m, 8H), 2.09 - 2.06 (m, 4H), 2.05 (s, 6H), 1.85 (s, 6H). ^{13}C NMR (100 MHz, $CDCl_3$) δ 178.69, 143.20, 139.38, 138.25, 136.28, 135.83, 135.64, 134.75, 134.03, 133.49, 126.69, 125.76, 118.25, 101.89, 38.55, 38.45, 29.84, 22.99, 15.39, 14.28. HRMS (MALDI-TOF) m/z: $[M + Na]^+$ Calcd for $C_{37}H_{33}BCl_2F_2NaO_2S_4$ 779.0699; Found 779.0702.

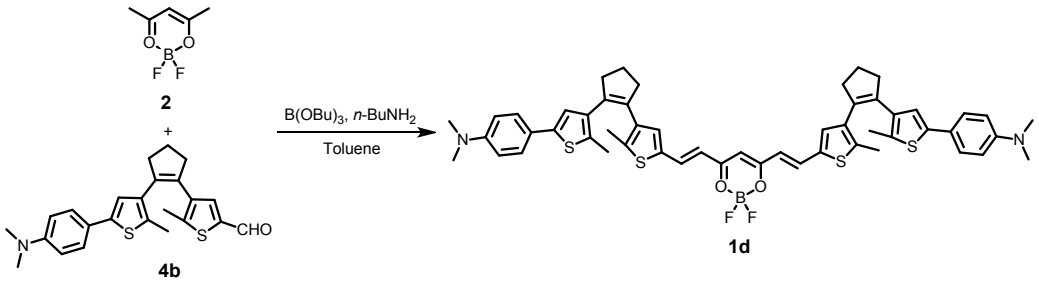

The solution of pentane-2, 4-dione (100 mg, 1.0 mmol) and $BF_3 \cdot OEt_2$ (0.13 mL, 1.0 mmol, 47%) in toluene (3 mL) is stirred at 65 °C for 2 h. Then the solution of intermediate **4b** (815 mg, 2.0 mmol) in toluene (4 mL) is added into the above reaction mixture, followed by $B(OBu)_3$ (0.81 mL, 3.0 mmol). The resulting solution is stirred for 30 min and *n*-butylamine (50 μL, 0.5 mmol) is slowly added, and stirred at 65 °C for 48 h. After cooling to room temperature, the solution is concentrated under reduced pressure and the residue is purified by column chromatography (silica gel: 200-300, PE : DCM = 1 : 5) to obtain the target compound **1d** as a brown solid (Yield: 43 %). ^{1}H NMR (400 MHz, $CDCl_3$) δ 7.98 (d, *J* = 15.1 Hz, 2H), 7.36 (d, *J* = 8.6 Hz, 4H), 7.14 (s, 2H), 6.81 (s, 2H), 6.69 (d, *J* = 8.7 Hz, 4H), 6.25 (d, *J* = 15.1 Hz, 2H), 5.87 (s, 1H), 2.95 (s, 12H), 2.83 - 2.78 (m, 8H), 2.11 - 2.04 (m, 4H), 2.02 (s, 6H), 1.94 (s, 6H). ^{13}C NMR (100 MHz, $CDCl_3$) δ 178.61, 149.99, 143.45, 141.14, 139.43, 138.74, 136.91, 136.07, 135.99, 135.91, 132.90, 132.43, 126.45, 123.09, 121.53, 118.07, 112.78, 101.75, 40.68, 38.64, 38.47, 23.10, 15.40, 14.42. HRMS (MALDI-TOF) m/z: $[M + Na]^+$ Calcd for $C_{53}H_{53}BF_2N_2NaO_2S_4$ 949.2949; Found 949.2948.

3. X-ray crystal structure data of 1a

Crystalline powder of complex **1a** suitable for X-ray structural analysis is obtained by slow evaporation of their chloroform / hexane mixed solutions. A crystal with approximate dimensions of 0.18 × 0.18 × 0.18 mm^3 for **1a** is mounted on a glass fiber for diffraction experiment. Intensity data are collected on a Nonius Kappa CCD diffractometer with MoKα radiation (0.71073 Å) at 293.43 (10) K. All non-H atoms are refined anisotropically. The hydrogen atoms were placed in the ideal positions and refined as riding atoms. Crystallographic data for the structure in this paper have been deposited with the Cambridge Crystallographic Data Centre as supplemental publication CCDC 1942422.

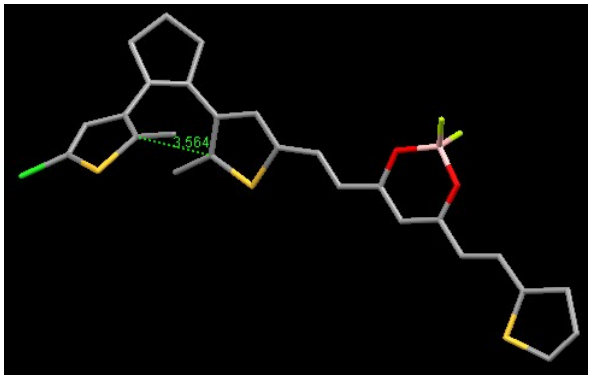

Figure S1. The intramolecular distance between the two reactive carbons of of dithienylethene **1a**.

Table S1. Crystal data and structure refinement for **1a.**

Identification code	**1a**
Empirical formula	$C_{26}H_{22}BClF_2O_2S_3$
Formula weight	546.87
Temperature/K	293.43(10)
Crystal system	triclinic
Space group	P-1
a/Å	8.0044(5)
b/Å	11.4822(8)
c/Å	16.6812(11)
α/°	80.569(6)
β/°	84.056(5)
γ/°	72.088(6)
Volume/Å^3	1436.80(17)
Z	2
ρ_{calc}g/cm^3	1.264
μ/mm^{-1}	0.384
F(000)	564.0
Crystal size/mm^3	0.18 × 0.18 × 0.18
Radiation	MoKα (λ = 0.71073)
2θ range for data collection/°	6.632 to 56.588
Index ranges	$-9 \le h \le 10$, $-12 \le k \le 14$, $-17 \le l \le 20$
Reflections collected	11315
Independent reflections	5979 [R_{int} = 0.0319, R_{sigma} = 0.0702]
Data/restraints/parameters	5979/0/321
Goodness-of-fit on F^2	1.321
Final R indexes [I>=2σ (I)]	R_1 = 0.1213, wR_2 = 0.3805
Final R indexes [all data]	R_1 = 0.1863, wR_2 = 0.4227
Largest diff. peak/hole / e Å^{-3}	1.77/-0.58

Table S2. Fractional Atomic Coordinates ($\times 10^4$) and Equivalent Isotropic Displacement Parameters ($Å^2 \times 10^3$) for **1a**. U_{eq} is defined as 1/3 of the trace of the orthogonalised U_{IJ} tensor.

Atom	*x*	*y*	*z*	U(eq)
S2	7244(2)	1749.5(15)	7713.9(10)	63.3(6)
S1	5565(3)	-1696(2)	10347.0(14)	100.4(9)
Cl1	7883(5)	-2727(2)	11723.1(14)	126.2(11)
S3	-1866(5)	9465(3)	4704.5(17)	143.5(14)
F2	4745(5)	3942(4)	3563(2)	83.4(13)
O1	4038(6)	3150(4)	4860(3)	65.2(12)
F1	2605(6)	3011(4)	3782(3)	87.2(14)
O2	2014(6)	4968(4)	4115(3)	64.1(12)
C24	-2166(16)	9329(9)	3166(10)	57(2)
C18	3894(7)	3777(5)	5476(4)	50.1(14)
C20	1882(7)	5535(5)	4747(4)	51.5(15)
C12	7516(8)	-57(6)	6968(4)	57.3(16)
C7	9344(8)	-1903(6)	7883(4)	55.8(16)
C11	8438(7)	-589(5)	7684(4)	51.5(15)
C17	4845(8)	3123(6)	6189(4)	54.4(15)
C21	697(8)	6775(6)	4697(4)	57.2(16)
C19	2847(8)	4971(6)	5430(4)	54.9(15)
C23	-1319(8)	8626(5)	3957(4)	57.2(16)
C22	-116(8)	7379(6)	4050(4)	59.4(16)
C13	6772(8)	1165(6)	6901(4)	55.0(15)
C14	8417(9)	307(6)	8149(4)	61.4(17)
C3	8157(9)	-2381(6)	9315(4)	60.9(17)
C16	5710(8)	1945(6)	6247(4)	56.2(15)
C6	9241(8)	-2662(6)	8573(4)	62.5(17)
C8	10591(9)	-2613(7)	7244(4)	70.9(19)
C2	8827(10)	-2780(6)	10104(4)	70.2(19)
C4	6346(9)	-1795(7)	9335(5)	76(2)
C1	7587(12)	-2457(7)	10698(5)	81(2)
C15	9320(11)	187(8)	8921(5)	82(2)
C5	5094(9)	-1313(8)	8664(5)	86(2)
C25	-3329(10)	10515(8)	3426(6)	89(3)
C10	10436(11)	-3942(7)	8515(5)	84(2)
B1	3373(11)	3758(7)	4056(5)	66(2)
C9	11078(13)	-3920(8)	7626(5)	106(3)
C26	-3185(15)	10691(8)	4142(6)	114(4)

Table S3. Anisotropic Displacement Parameters ($Å^2 \times 10^3$) for **1a**. The Anisotropic displacement factor exponent takes the form: $-2\pi^2[h^2a^{*2}U_{11}+2hka^*b^*U_{12}+\ldots]$.

Atom	U_{11}	U_{22}	U_{33}	U_{23}	U_{13}	U_{12}
S2	77.8(12)	56.7(11)	51.5(11)	-7.0(8)	-3.3(8)	-14.8(8)
S1	108.3(17)	85.5(15)	72.2(15)	5.1(12)	29.5(12)	3.4(12)
Cl1	215(3)	95.5(17)	56.5(14)	-9.7(13)	5.1(16)	-33.7(18)
S3	200(3)	93.3(19)	83.5(19)	-21.6(15)	-13.2(19)	42.1(19)
F2	73(3)	94(3)	67(3)	-9(2)	8(2)	-6(2)
O1	76(3)	50(3)	54(3)	-8(2)	-15(2)	9(2)
F1	99(3)	65(3)	101(4)	-26(2)	-37(3)	-12(2)
O2	72(3)	51(3)	58(3)	-9(2)	-17(2)	2.7(19)
C24	50(3)	37(4)	80(5)	-16(4)	-10(3)	-2(3)
C18	45(3)	48(3)	53(4)	-6(3)	1(2)	-9(2)
C20	47(3)	47(3)	53(4)	-9(3)	6(3)	-6(2)
C12	73(4)	59(4)	37(3)	-7(3)	0(3)	-18(3)
C7	52(3)	64(4)	51(4)	-7(3)	-5(3)	-16(3)
C11	52(3)	50(4)	51(4)	-4(3)	2(3)	-17(3)
C17	57(3)	63(4)	44(3)	-14(3)	3(3)	-17(3)
C21	54(3)	52(4)	60(4)	-9(3)	-1(3)	-7(3)
C19	59(4)	51(4)	53(4)	-15(3)	2(3)	-11(3)
C23	51(3)	47(3)	68(4)	-6(3)	5(3)	-11(3)
C22	58(4)	52(4)	64(4)	-8(3)	2(3)	-12(3)
C13	62(4)	57(4)	39(3)	0(3)	6(3)	-14(3)
C14	72(4)	66(4)	45(4)	0(3)	-6(3)	-22(3)
C3	74(4)	50(3)	47(4)	2(3)	2(3)	-8(3)
C16	58(4)	58(4)	48(4)	-3(3)	-2(3)	-13(3)
C6	60(4)	62(4)	56(4)	-2(3)	1(3)	-8(3)

Table S4. Bond Lengths for **1a**.

Atom	Atom	Length/Å	Atom	Atom	Length/Å
S2	C13	1.729(7)	C12	C13	1.336(9)
S2	C14	1.715(7)	C7	C11	1.458(8)
S1	C4	1.747(7)	C7	C6	1.337(9)
S1	C1	1.698(9)	C7	C8	1.536(9)
Cl1	C1	1.714(8)	C11	C14	1.381(9)
S3	C23	1.642(7)	C17	C16	1.309(9)
S3	C26	1.683(10)	C21	C22	1.300(9)
F2	B1	1.352(9)	C23	C22	1.453(9)
O1	C18	1.324(7)	C13	C16	1.456(9)
O1	B1	1.477(9)	C14	C15	1.508(10)
F1	B1	1.354(9)	C3	C6	1.459(9)
O2	C20	1.306(7)	C3	C2	1.424(9)
O2	B1	1.488(8)	C3	C4	1.397(10)
C24	C23	1.534(18)	C6	C10	1.499(9)
C24	C25	1.497(14)	C8	C9	1.480(10)
C18	C17	1.449(9)	C2	C1	1.340(10)
C18	C19	1.365(8)	C4	C5	1.501(11)
C20	C21	1.442(8)	C25	C26	1.266(12)
C20	C19	1.395(9)	C10	C9	1.516(10)
C12	C11	1.418(8)			

Table S5. Bond Angles for **1a**.

Atom	Atom	Atom	Angle/°	Atom	Atom	Atom	Angle/°
C14	S2	C13	91.9(3)	C11	C14	S2	111.4(5)
C1	S1	C4	92.3(4)	C11	C14	C15	129.6(6)
C23	S3	C26	94.0(4)	C15	C14	S2	118.8(5)
C18	O1	B1	122.1(5)	C2	C3	C6	122.6(6)
C20	O2	B1	120.6(5)	C4	C3	C6	124.1(7)
C25	C24	C23	102.6(11)	C4	C3	C2	113.1(6)
O1	C18	C17	116.9(5)	C17	C16	C13	128.7(7)
O1	C18	C19	120.0(6)	C7	C6	C3	128.3(6)
C19	C18	C17	123.1(6)	C7	C6	C10	111.1(6)
O2	C20	C21	116.4(6)	C3	C6	C10	120.5(6)
O2	C20	C19	121.6(5)	C9	C8	C7	104.6(6)
C19	C20	C21	122.0(6)	C1	C2	C3	112.4(7)
C13	C12	C11	114.8(6)	C3	C4	S1	108.9(6)
C11	C7	C8	120.3(6)	C3	C4	C5	131.1(7)
C6	C7	C11	129.2(6)	C5	C4	S1	120.0(5)
C6	C7	C8	110.5(6)	S1	C1	Cl1	120.2(5)
C12	C11	C7	124.1(6)	C2	C1	S1	113.3(6)
C14	C11	C12	111.0(5)	C2	C1	Cl1	126.6(7)
C14	C11	C7	124.8(6)	C26	C25	C24	116.5(9)
C16	C17	C18	121.8(6)	C6	C10	C9	104.7(6)
C22	C21	C20	124.4(6)	F2	B1	O1	108.1(6)
C18	C19	C20	120.7(6)	F2	B1	F1	112.8(7)
C24	C23	S3	112.2(5)	F2	B1	O2	109.2(6)
C22	C23	S3	122.5(6)	O1	B1	O2	111.5(6)
C22	C23	C24	125.3(7)	F1	B1	O1	107.4(6)
C21	C22	C23	127.2(7)	F1	B1	O2	107.8(6)
C12	C13	S2	110.7(5)	C8	C9	C10	107.5(6)
C12	C13	C16	126.7(6)	C25	C26	S3	114.2(7)
C16	C13	S2	122.6(5)				

Table S6. Hydrogen Atom Coordinates (Å×10^4) and Isotropic Displacement Parameters (Å^2×10^3) for **1a**.

Atom	*x*	*y*	*z*	U(eq)
H24	-2210(180)	9290(110)	3140(100)	68
H12	7434	-523	6576	69
H17	4841	3552	6616	65
H21	502	7168	5157	69
H19	2775	5415	5858	66
H22	95	6968	3597	71
H16	5636	1553	5812	67
H8A	10004	-2509	6745	85
H8B	11624	-2329	7121	85
H2	9995	-3215	10197	84
H15A	9492	963	8970	123
H15B	10439	-436	8906	123
H15C	8603	-44	9381	123
H5A	3991	-1463	8847	129
H5B	5578	-1728	8200	129
H5C	4910	-441	8516	129
H25	-4117	11094	3079	107
H10A	9804	-4549	8674	101
H10B	11415	-4137	8861	101
H9A	12343	-4286	7580	128
H9B	10533	-4388	7359	128
H26	-3757	11432	4340	137

4. Photochromism and fluorescent switching behaviors of 1a-1d

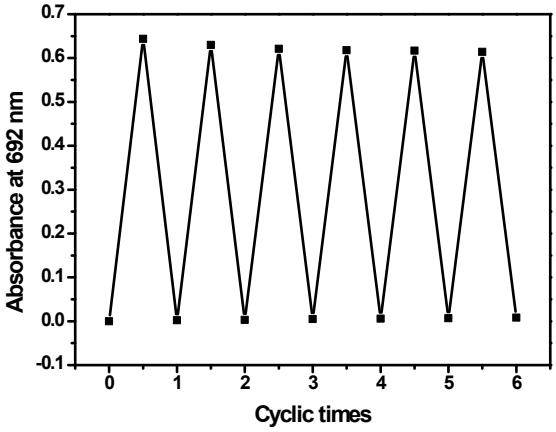

Figure S2. Fatigue resistance of **1a** on alternating irradiation with green light at 520 - 530 nm and red light at 650 - 660 nm over six cycles in toluene (2.0 × 10^{-5} mol/L).

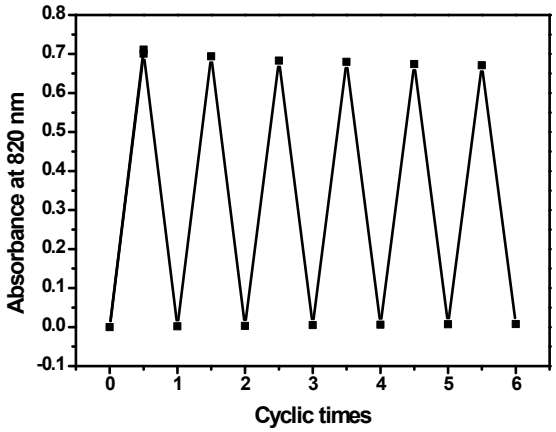

Figure S3. Fatigue resistance of **1b** on alternating irradiation with green light at 520 - 530 nm and near-infrared light at 800 - 810 nm over six cycles in toluene (2.0×10^{-5} mol/L).

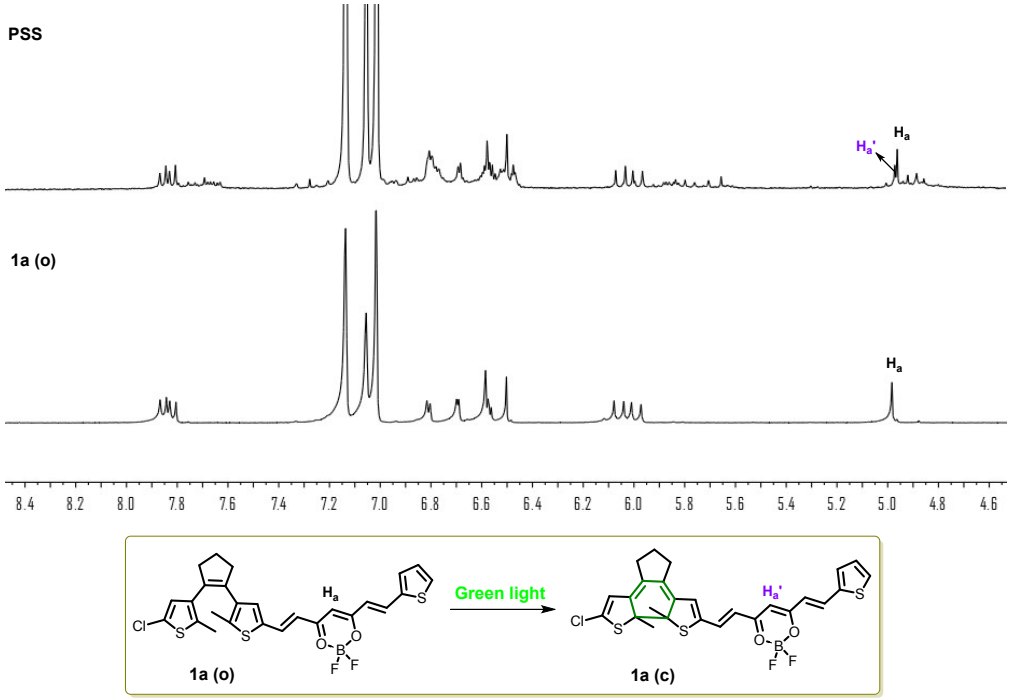

Figure S4. Partial ^{1}H NMR spectral changes of **1a** upon irradiation with green light at 520 - 530 nm in toluene-d_8 at room temperature.

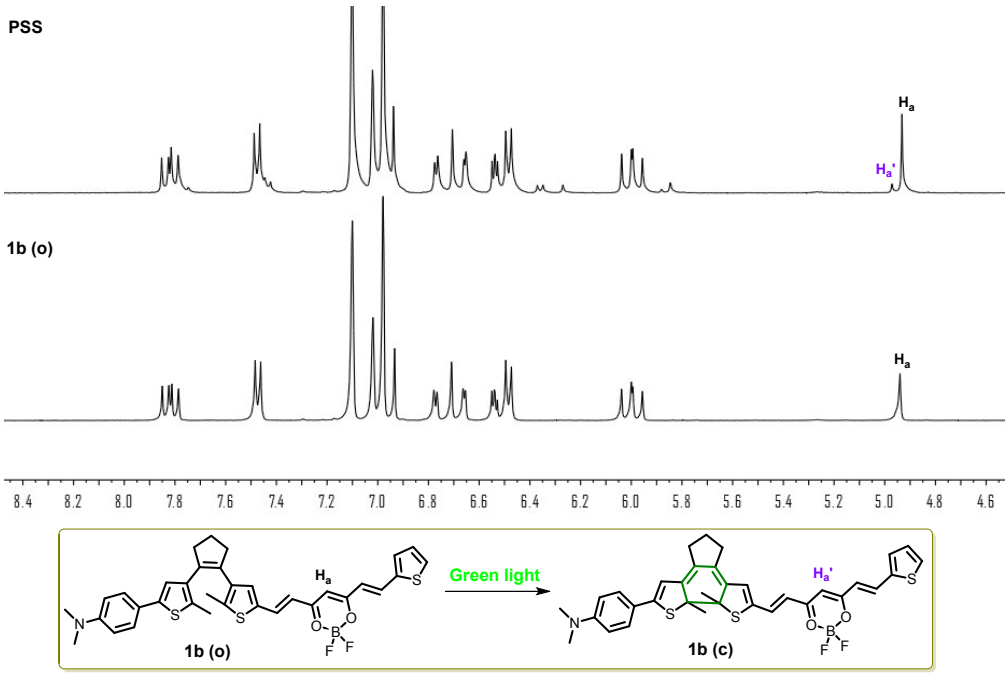

Figure S5. Partial ^{1}H NMR spectral changes of **1b** upon irradiation with green light at 520 - 530 nm in toluene-d_8 at room temperature.

Table S7. The conversion ratio of **1a-1d** at the photostationary state (PSS).

Compounds	Conversion ratio (%)	Compounds	Conversion ratio (%)
1a	42	**1c**	51
1b	19	**1d**	34

Table S8. The fluorescence data of **1a-1d** in toluene (2.0×10^{-5} mol/L).

Solvents	$\lambda_{em}{}^{a}$ (nm)	$\Phi_f{}^{b}$	Rate of quenching (%)^{c}
1a	550	0.49	75
1b	556	0.17	84
1c	552	0.37	65
1d	582	0.14	82

[a] Fluorescence emission maxima; [b] Fluorescence quantum yield determined by a standard method with rhodamine 6G in water ($\Phi_f = 0.75$, $\lambda_{ex} = 488$ nm) as reference; [c] Percentage of fluorescence intensity quenching upon irradiation with green light (520 - 530 nm).

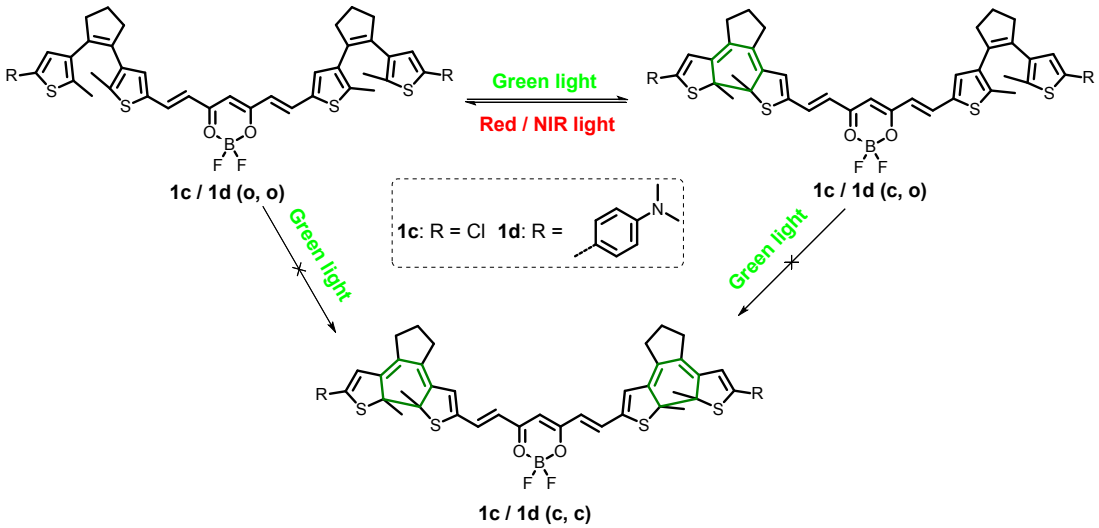

Scheme S2. Photochromic reaction of bis-dithienylethenes **1c** and **1d**.

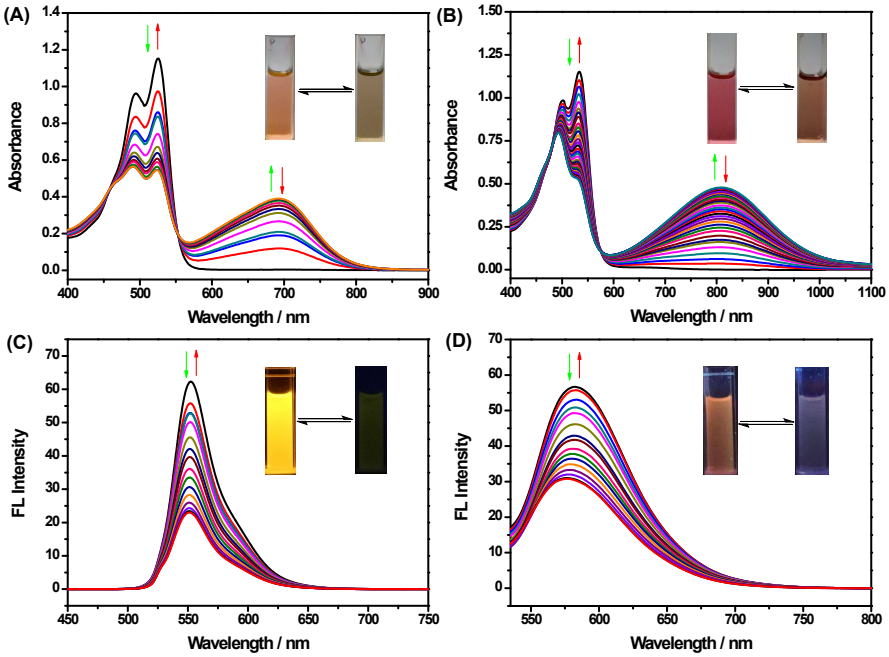

Figure S6. The absorption and emission spectra changes of **1c** and **1d** in toluene (2.0×10^{-5} mol/L) upon alternating irradiation with green light at 520 - 530 nm and red light at 650 - 660 nm (or near-infrared light at 800 - 810 nm). (Inset) Corresponding color and fluorescence changes of **1c** and **1d** upon photoirradiation, (A) absorption spectra changes for **1c** (0 - 55 s); (B) absorption spectra changes for **1d** (0 - 1200 s); (C) emission spectra changes for **1c**; (D) emission spectra changes for **1d**.

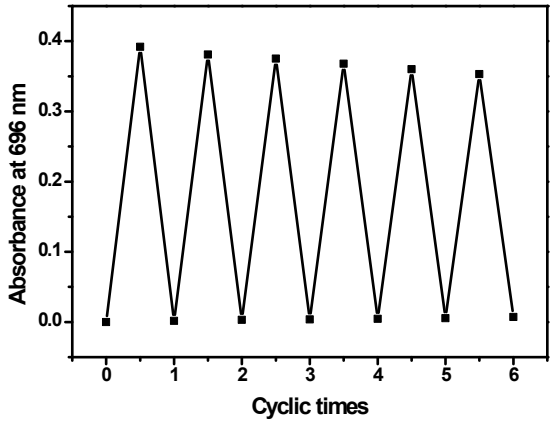

Figure S7. Fatigue resistance of **1c** on alternating irradiation with green light at 520 - 530 nm and red light at 650 - 660 nm over six cycles in toluene (2.0×10^{-5} mol/L).

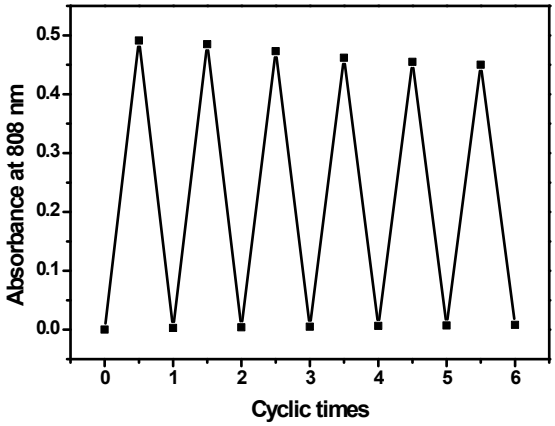

Figure S8. Fatigue resistance of **1d** on alternating irradiation with green light at 520 - 530 nm and near-infrared light at 800 - 810 nm over six cycles in toluene (2.0×10^{-5} mol/L).

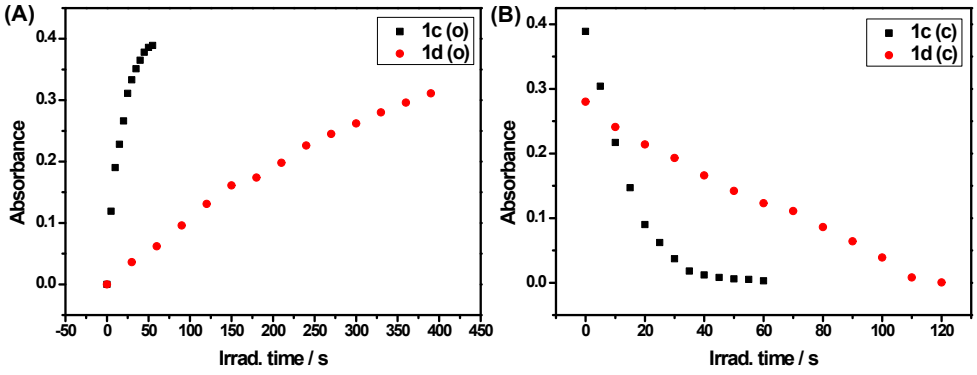

Figure S9. Optical response rates of **1c** and **1d** upon irradiation with green light (A) and red / NIR light (B) in toluene monitored at the maximum absorption wavelength for ring-closed isomers.

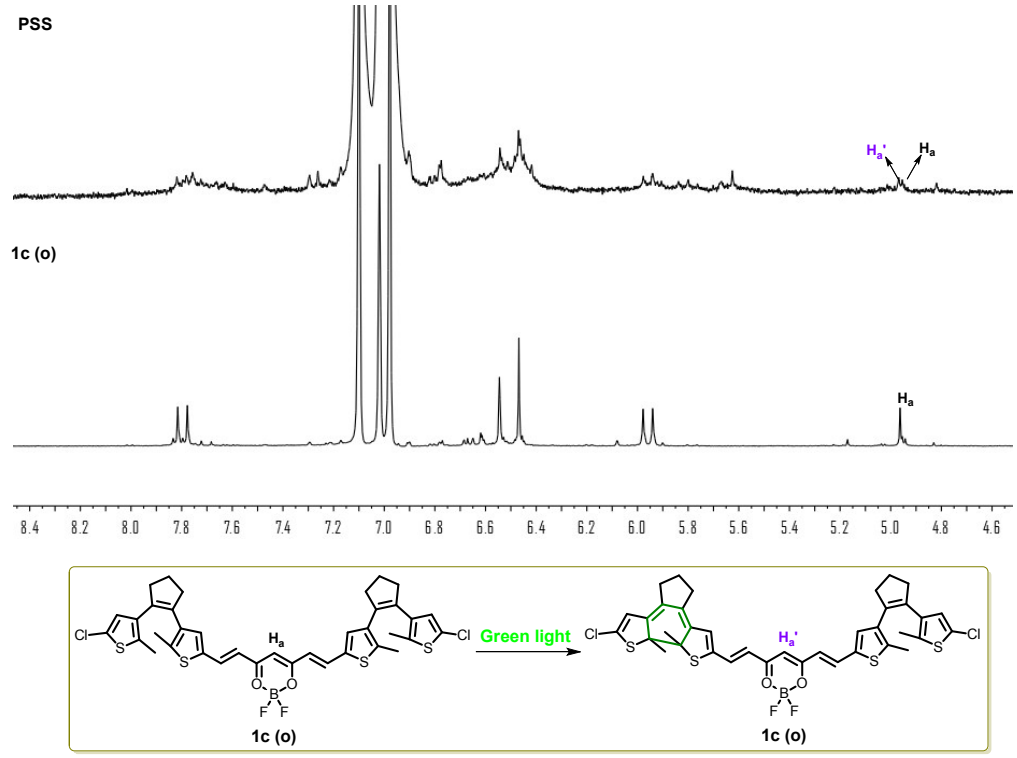

Figure S10. Partial ^{1}H NMR spectral changes of **1c** upon irradiation with green light at 520 - 530 nm in toluene-d_8 at room temperature (Note: solubility of **1c** becomes worse after irradiation with green light).

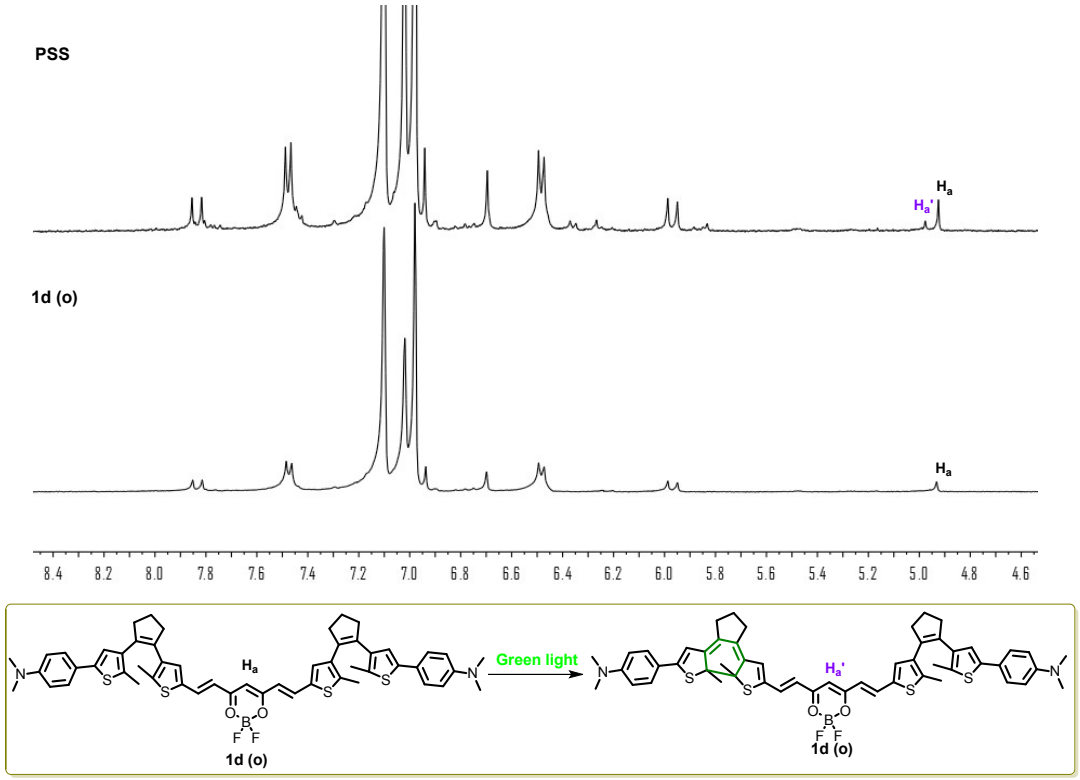

Figure S11. Partial ^{1}H NMR spectral changes of **1d** upon irradiation with green light at 520 - 530 nm in toluene-d_8 at room temperature.

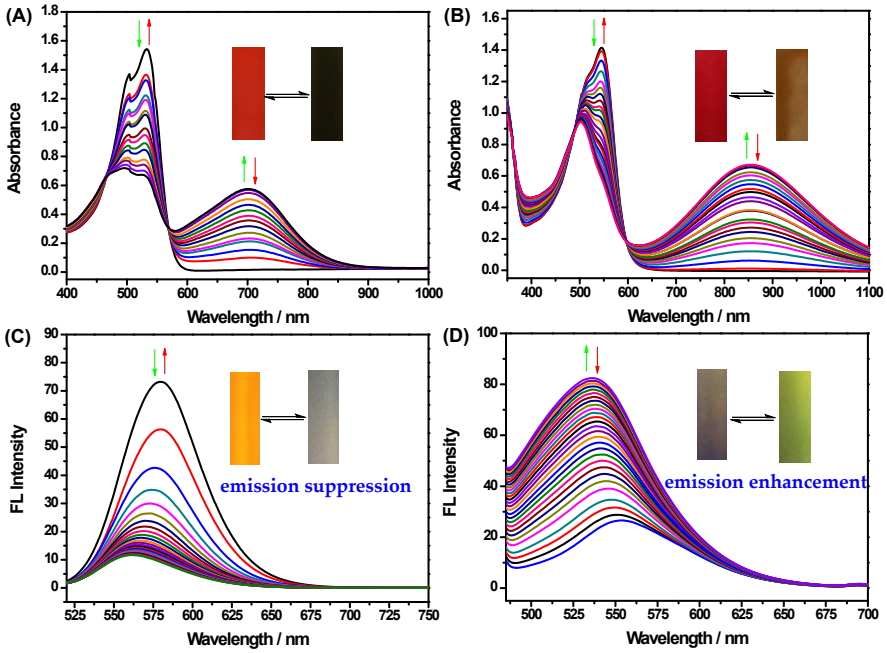

Figure S12. The absorption and emission spectra changes of **1c** and **1d** in the PMMA film upon alternating irradiation with green light at 520 - 530 nm and red light at 650 - 660 nm (or near-infrared light at 800 - 810 nm). (Inset) Corresponding color and fluorescence changes of **1c** and **1d** upon photoirradiation, (A) absorption spectra changes for **1c** (0 - 30 s); (B) absorption spectra changes for **1d** (0 - 57 s); (C) emission spectra changes for **1c**; (D) emission spectra changes for **1d**.

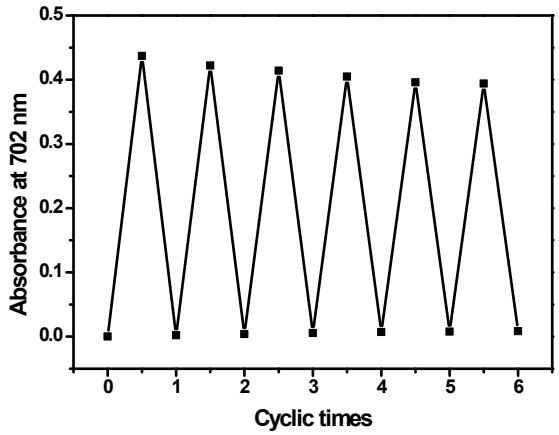

Figure S13. Fatigue resistance of **1a** on alternating irradiation with green light at 520 - 530 nm and red light at 650 - 660 nm over six cycles in the PMMA film.

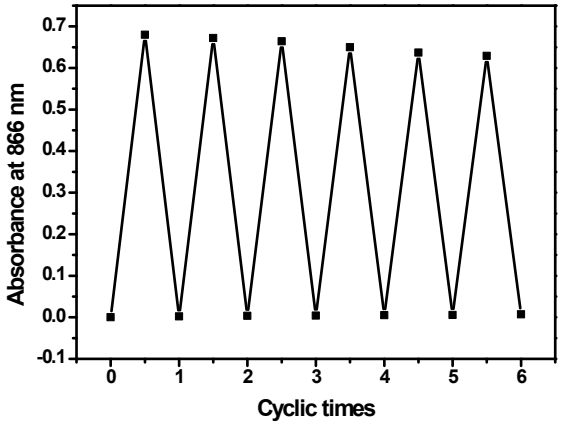

Figure S14. Fatigue resistance of **1b** on alternating irradiation with green light at 520 - 530 nm and near-infrared light at 800 - 810 nm over six cycles in the PMMA film.

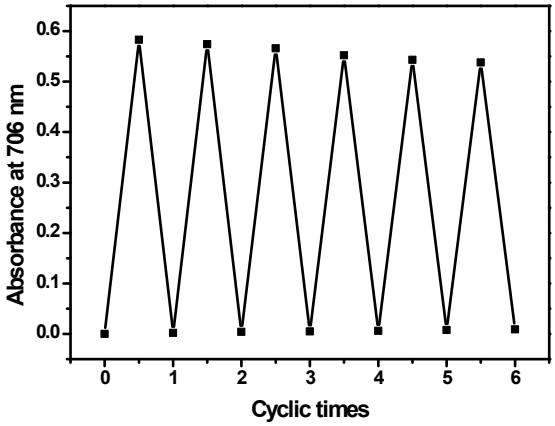

Figure S15. Fatigue resistance of **1c** on alternating irradiation with green light at 520 - 530 nm and red light at 650 - 660 nm over six cycles in the PMMA film.

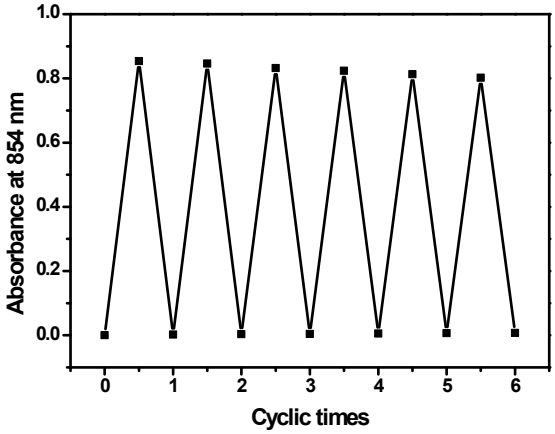

Figure S16. Fatigue resistance of **1d** on alternating irradiation with green light at 520 - 530 nm and near-infrared light at 800 - 810 nm over six cycles in the PMMA film.

5. DFT theoretical calculations of 1a-1d

The electron densities and ground-state geometries of **1a-1d** are calculated via density functional theory in Gaussian 09 B3LYP/6-31G* level.[4-6]

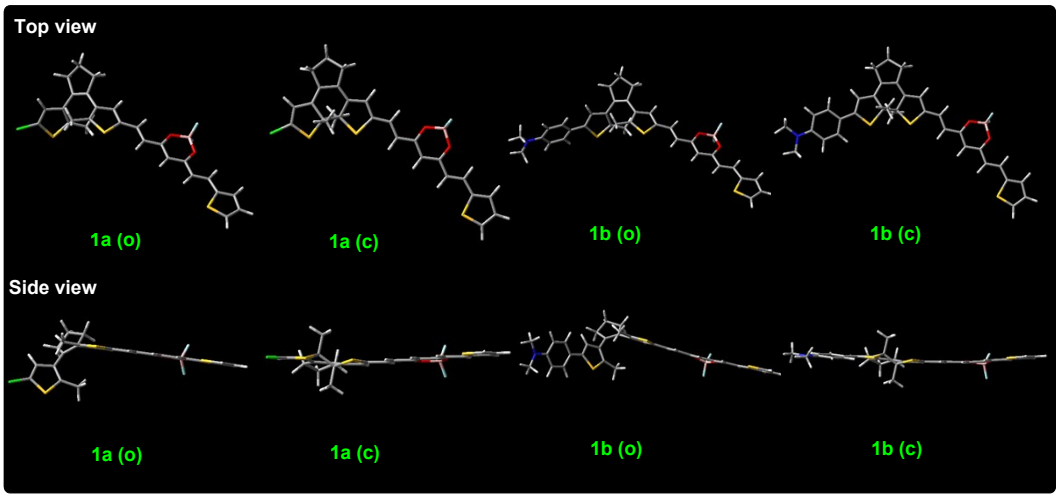

Figure S17. Optimized ground-state geometry of **1a** and **1b** based on DFT calculations at the B3LYP/6-31G* level by using the Gaussian 09 program.

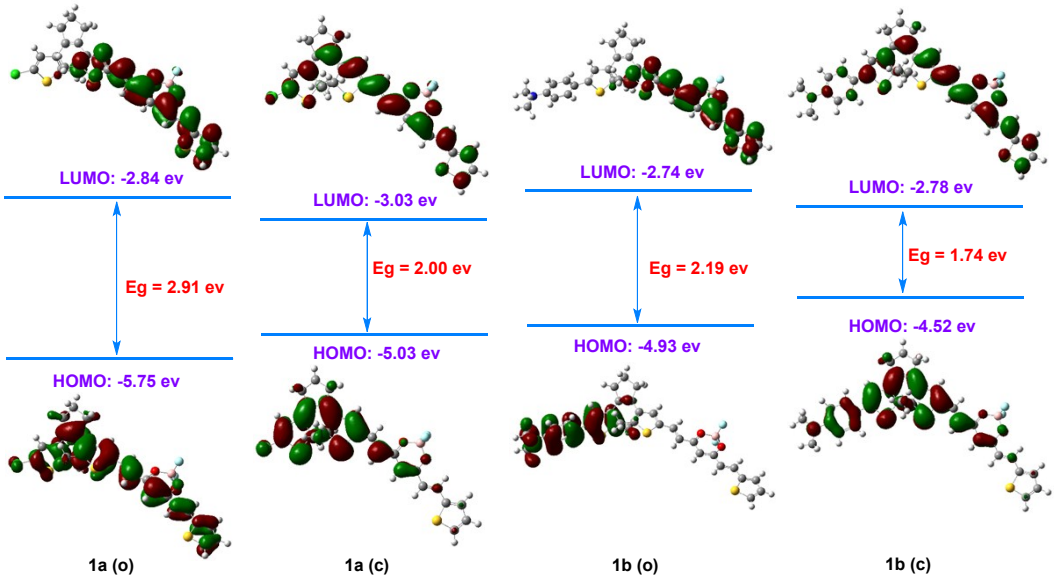

Figure S18. Frontier molecular orbital profiles of **1a** and **1b** based on DFT calculations at the B3LYP/6-31G* level by using the Gaussian 09 program.

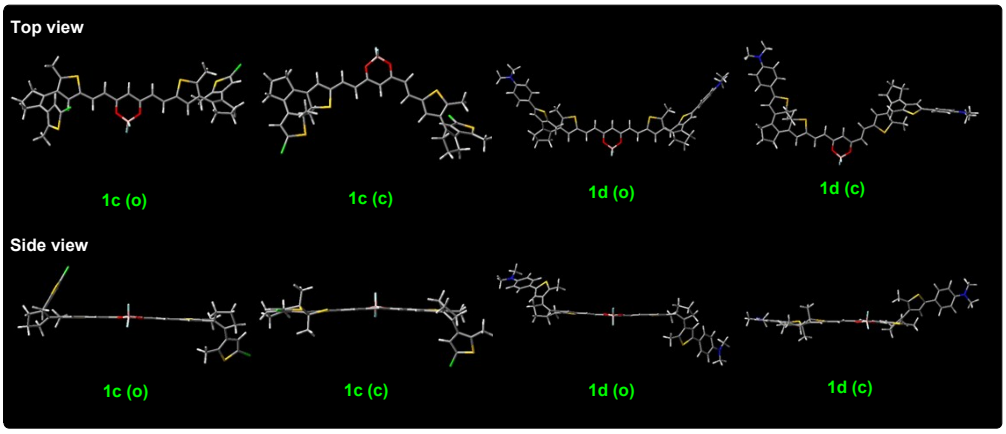

Figure S19. Optimized ground-state geometry of **1c** and **1d** based on DFT calculations at the B3LYP/6-31G* level by using the Gaussian 09 program.

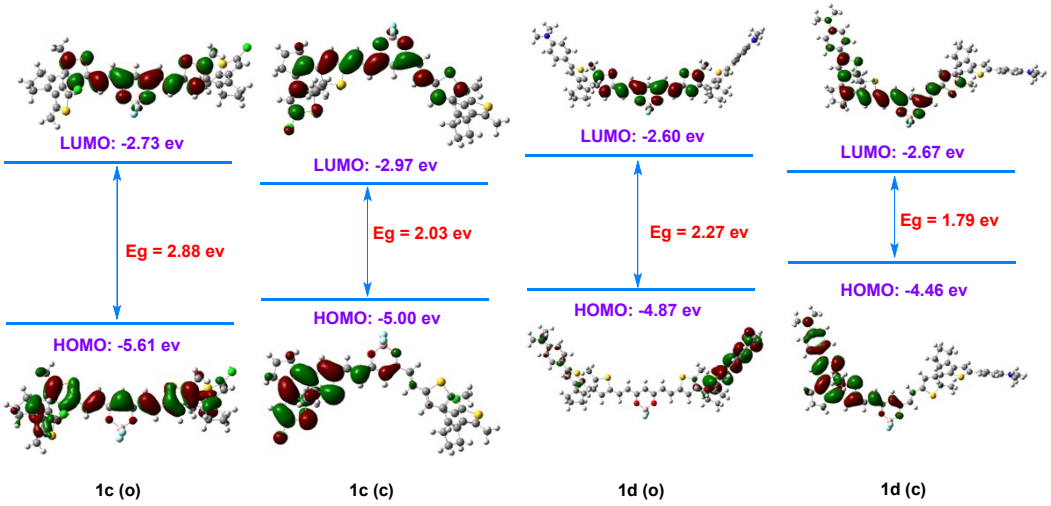

Figure S20. Frontier molecular orbital profiles of **1c** and **1d** based on DFT calculations at the B3LYP/6-31G* level by using the Gaussian 09 program.

6. Confocal fluorescence microscope imaging of 1b

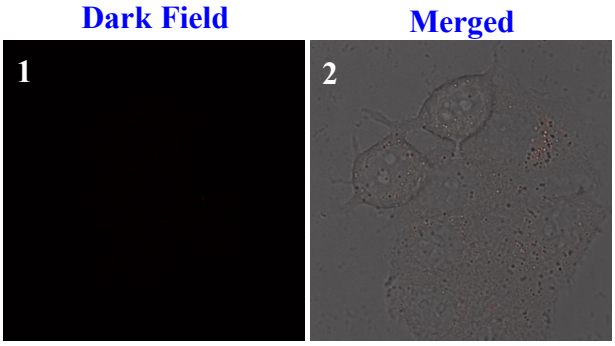

Figure S21. Fluorescence and bright-field images of cells are stained with **1b** (10 μM) before irradiation with green light at 520 - 530 nm (λ_{ex} = 510 nm, λ_{em} = 530 - 750 nm). Fluoresce image (1); merged images of fluorescence and bright fields (2).

7. Appendix: NMR and Mass spectra

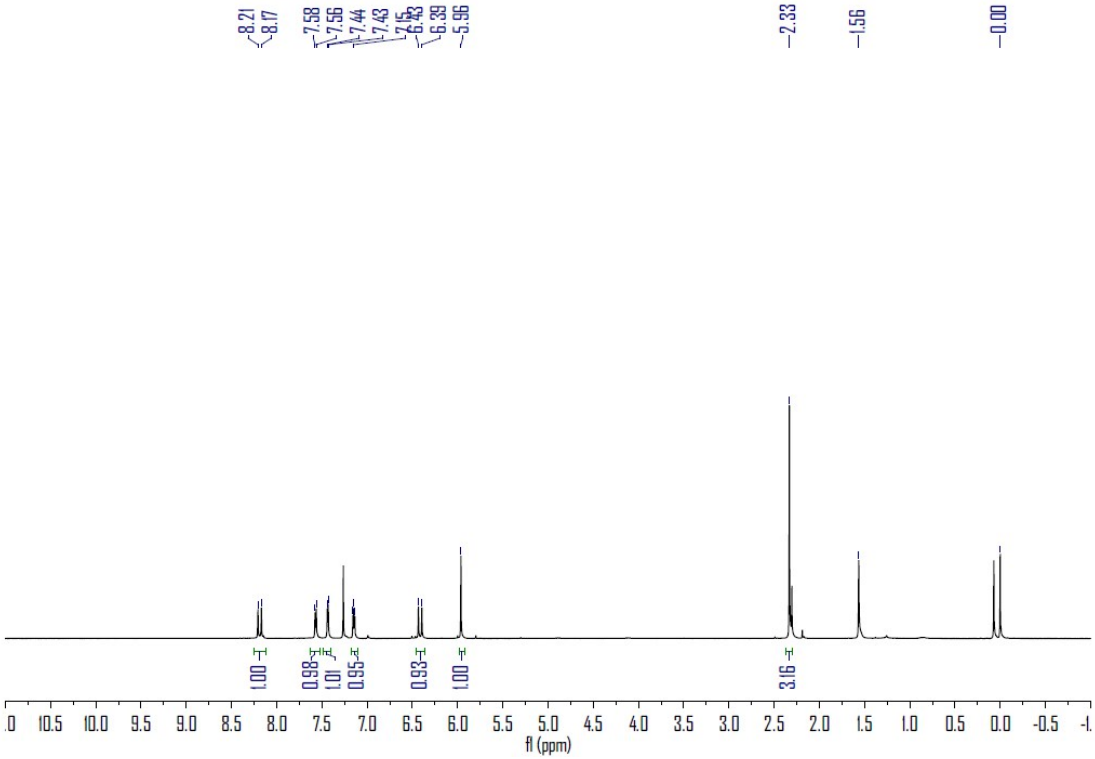

Figure S22. 400 MHz ^{1}H NMR spectrum of **3** in $CDCl_3$ at room temperature.

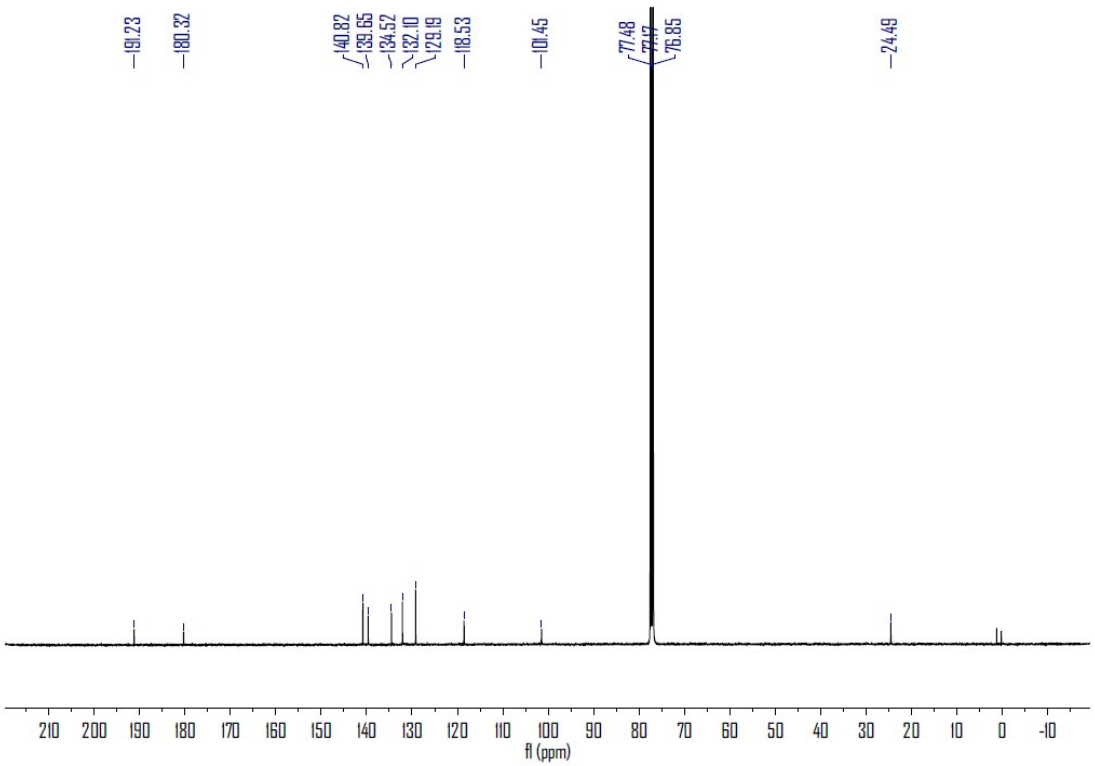

Figure S23. 100 MHz ^{13}C NMR spectrum of **3** in $CDCl_3$ at room temperature.

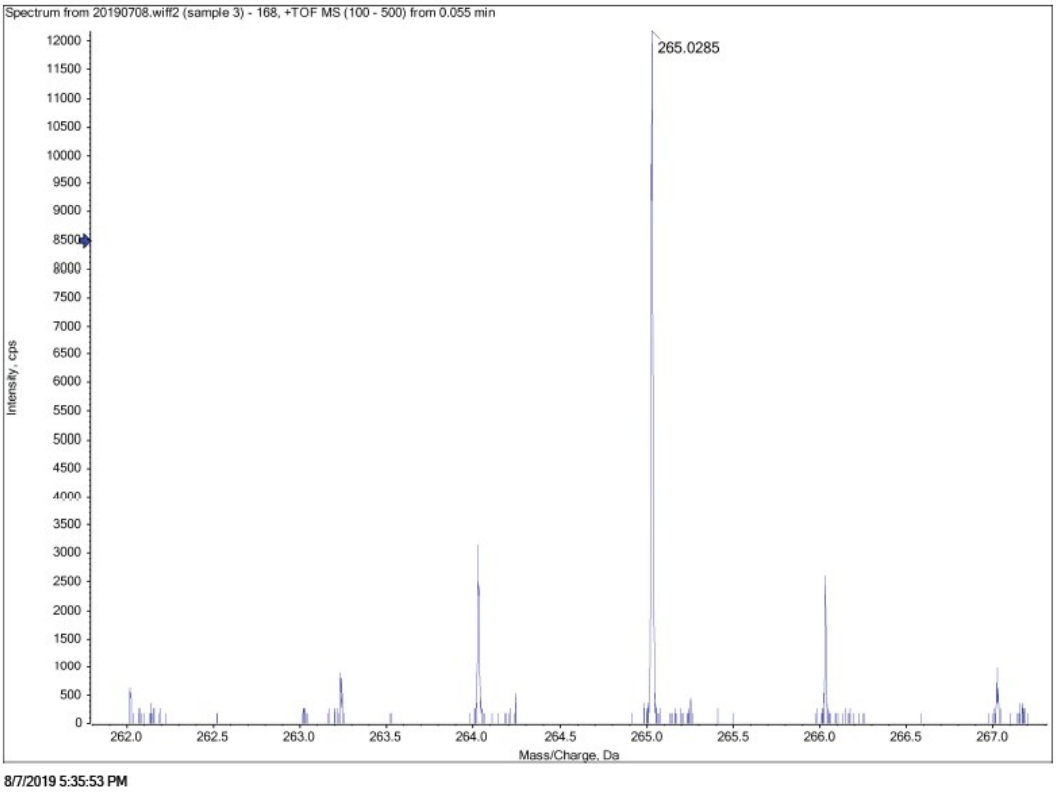

Figure S24. HRMS of **3**.

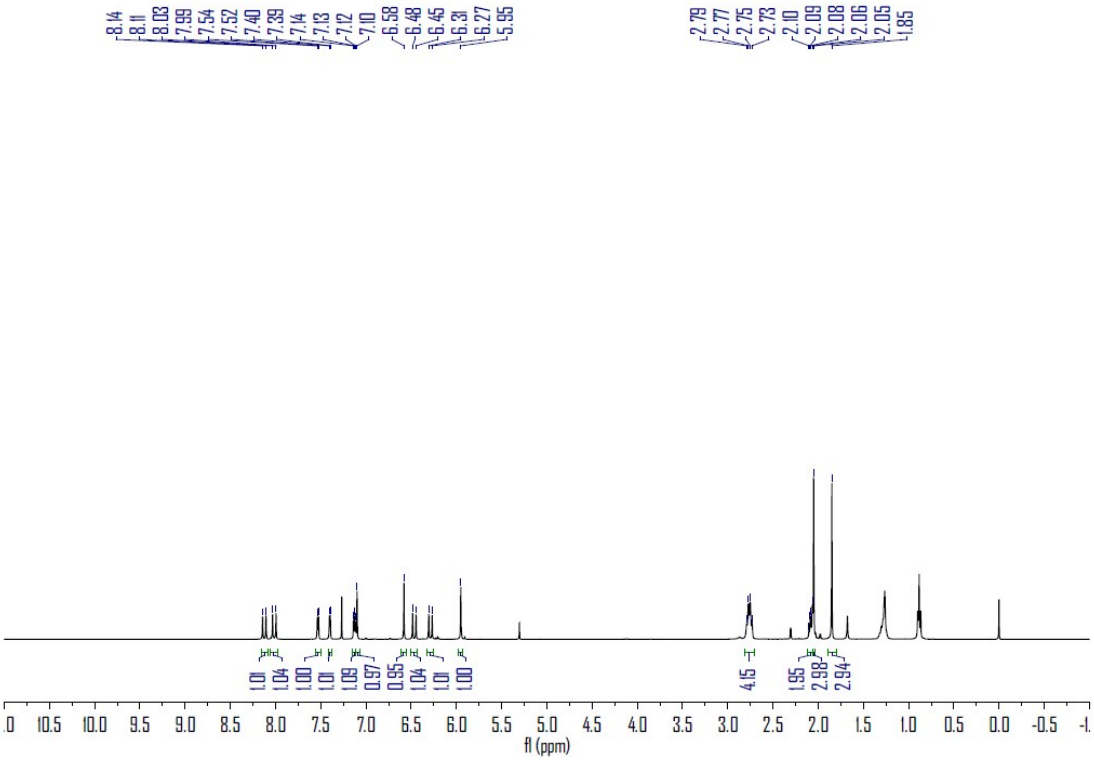

Figure S25. 400 MHz ^{1}H NMR spectrum of **1a** in $CDCl_3$ at room temperature.

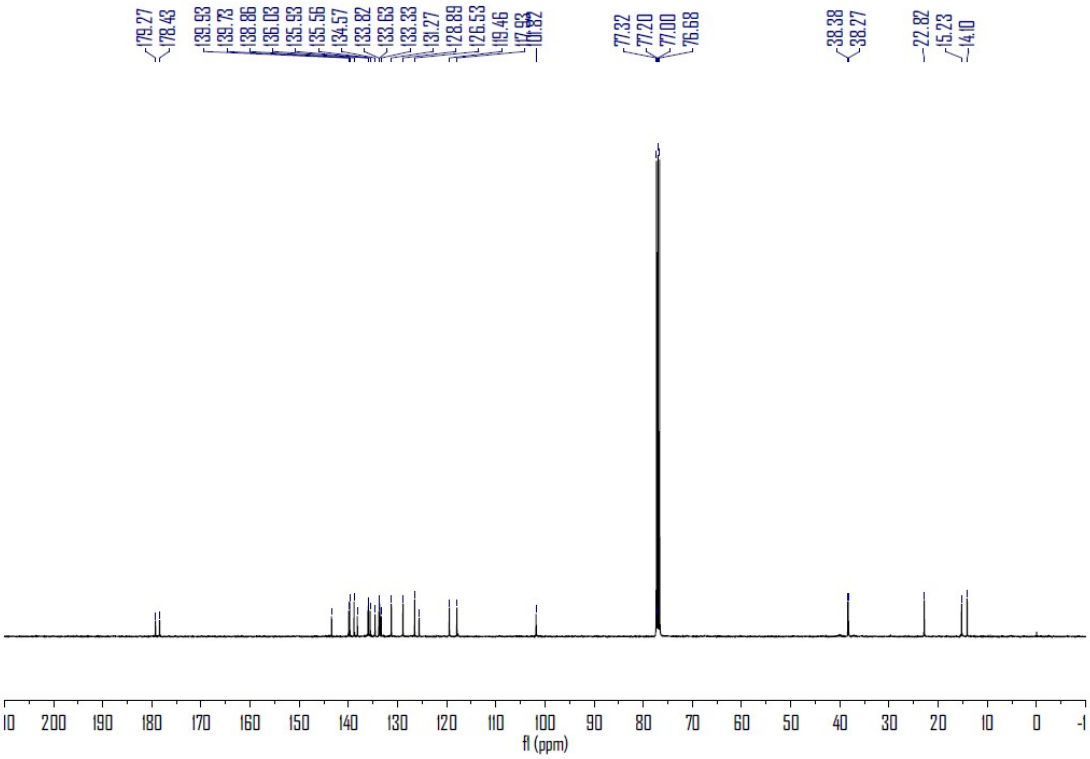

Figure S26. 100 MHz ^{13}C NMR spectrum of **1a** in $CDCl_3$ at room temperature.

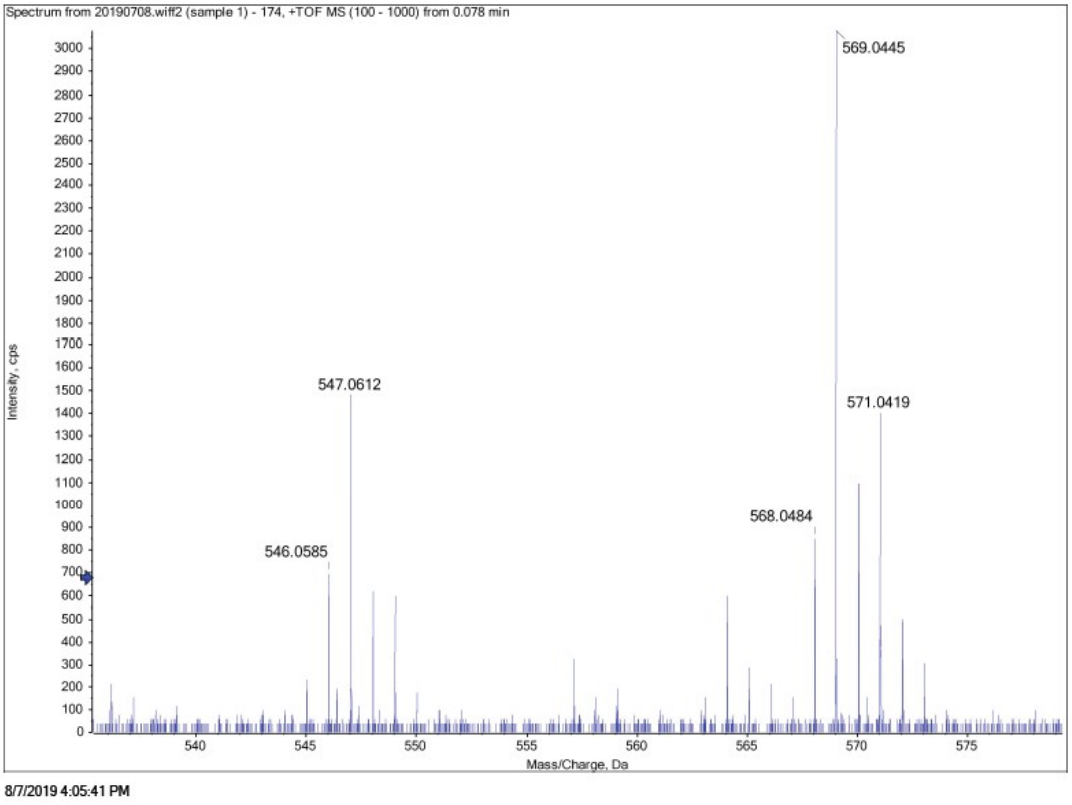

Figure S27. HRMS of **1a**.

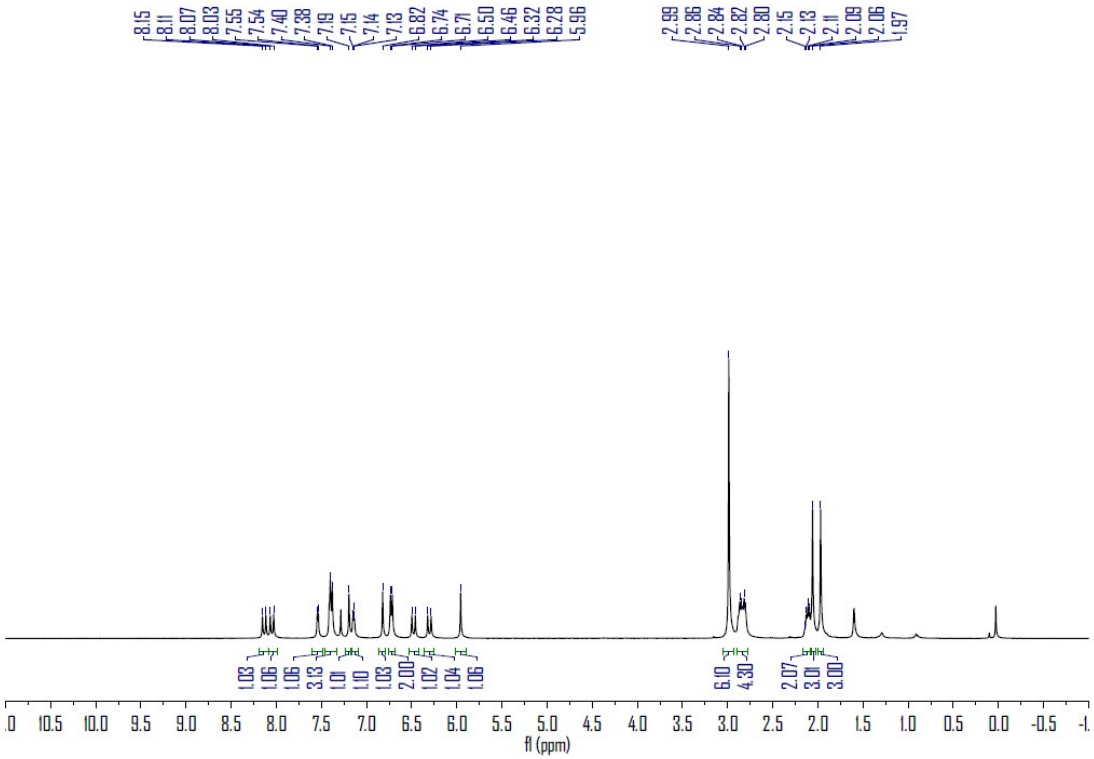

Figure S28. 400 MHz ^{1}H NMR spectrum of **1b** in $CDCl_3$ at room temperature.

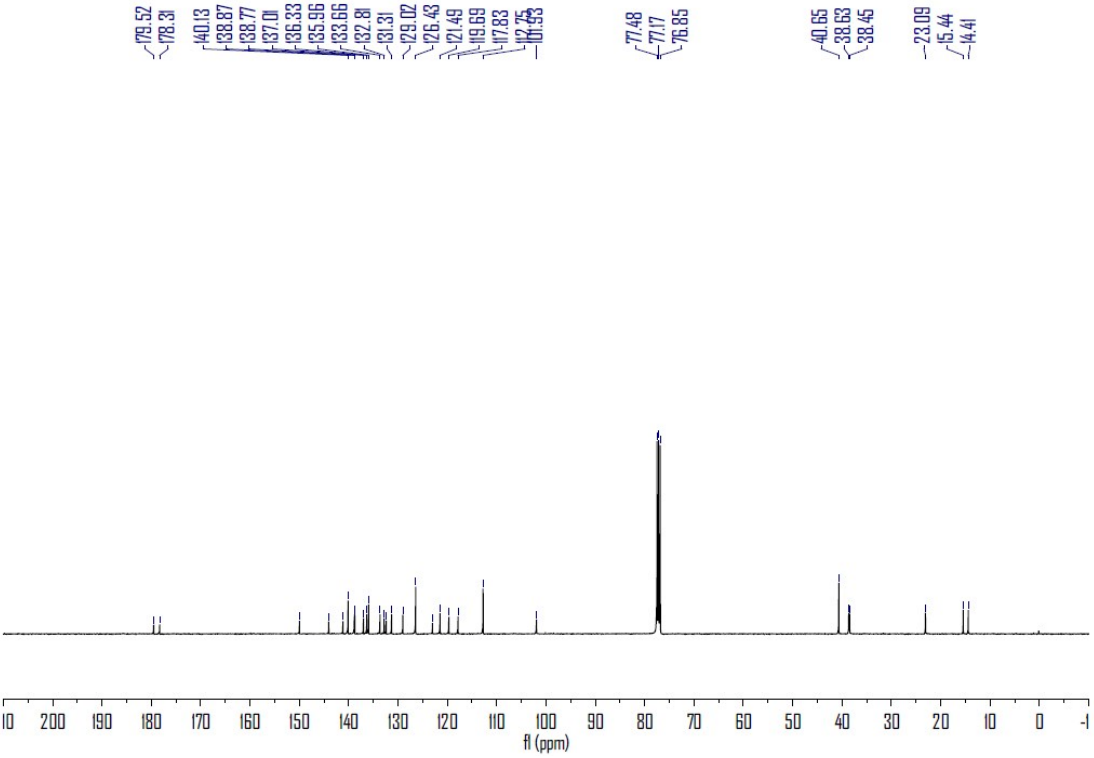

Figure S29. 100 MHz ^{13}C NMR spectrum of **1b** in $CDCl_3$ at room temperature.

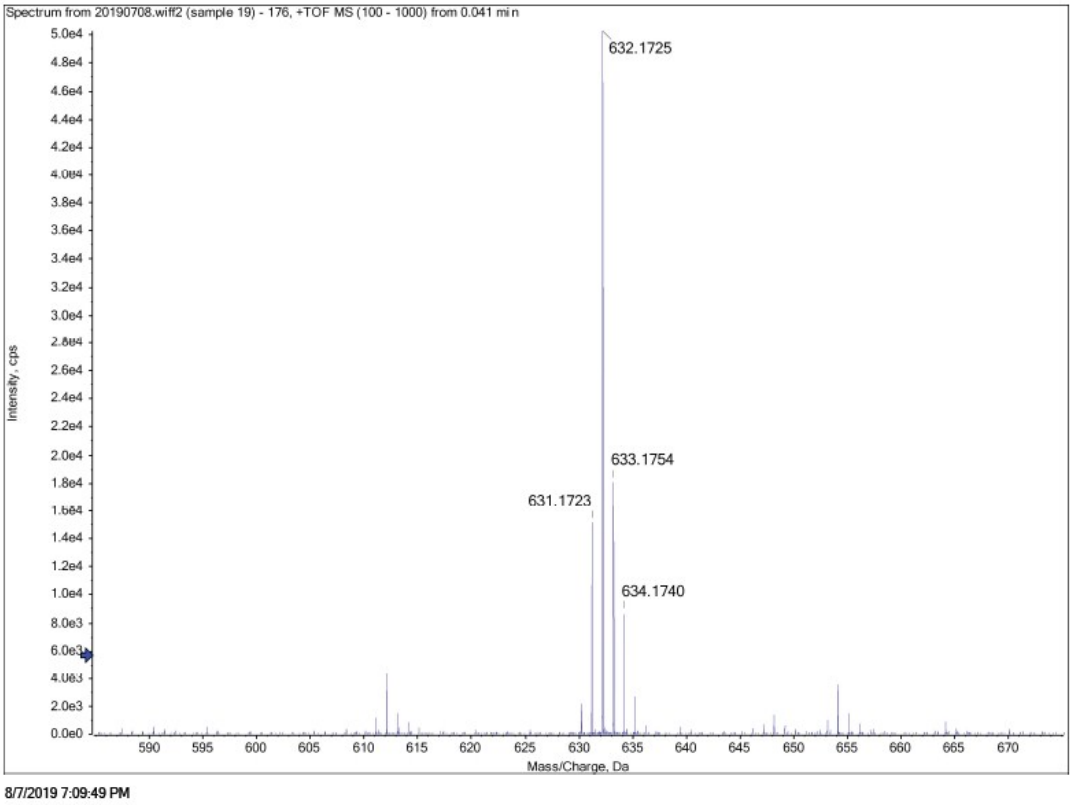

Figure S30. HRMS of **1b**.

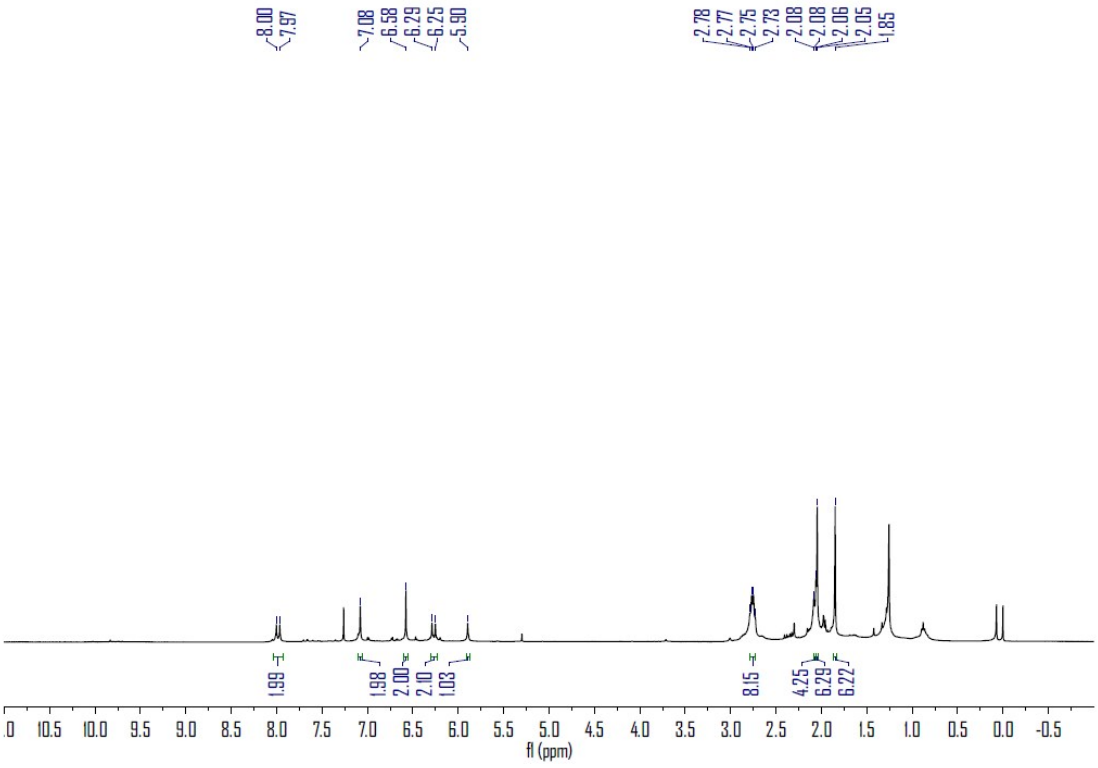

Figure S31. 400 MHz ^{1}H NMR spectrum of **1c** in $CDCl_3$ at room temperature.

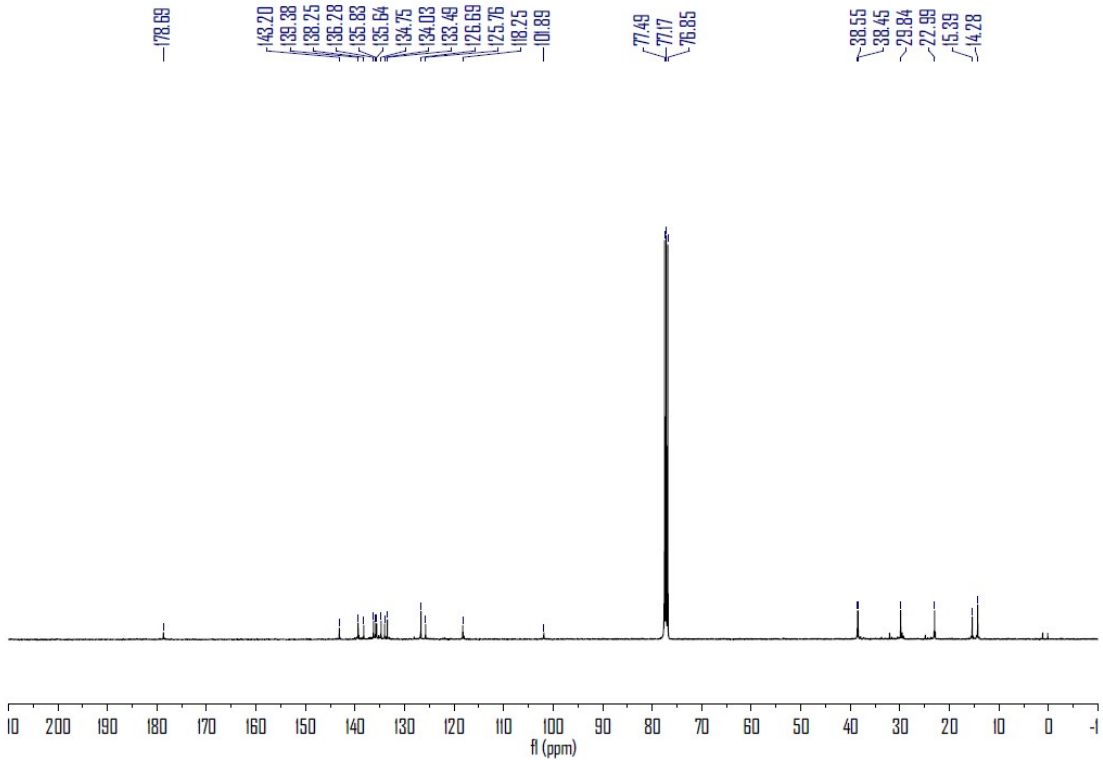

Figure S32. 100 MHz ^{13}C NMR spectrum of **1c** in $CDCl_3$ at room temperature.

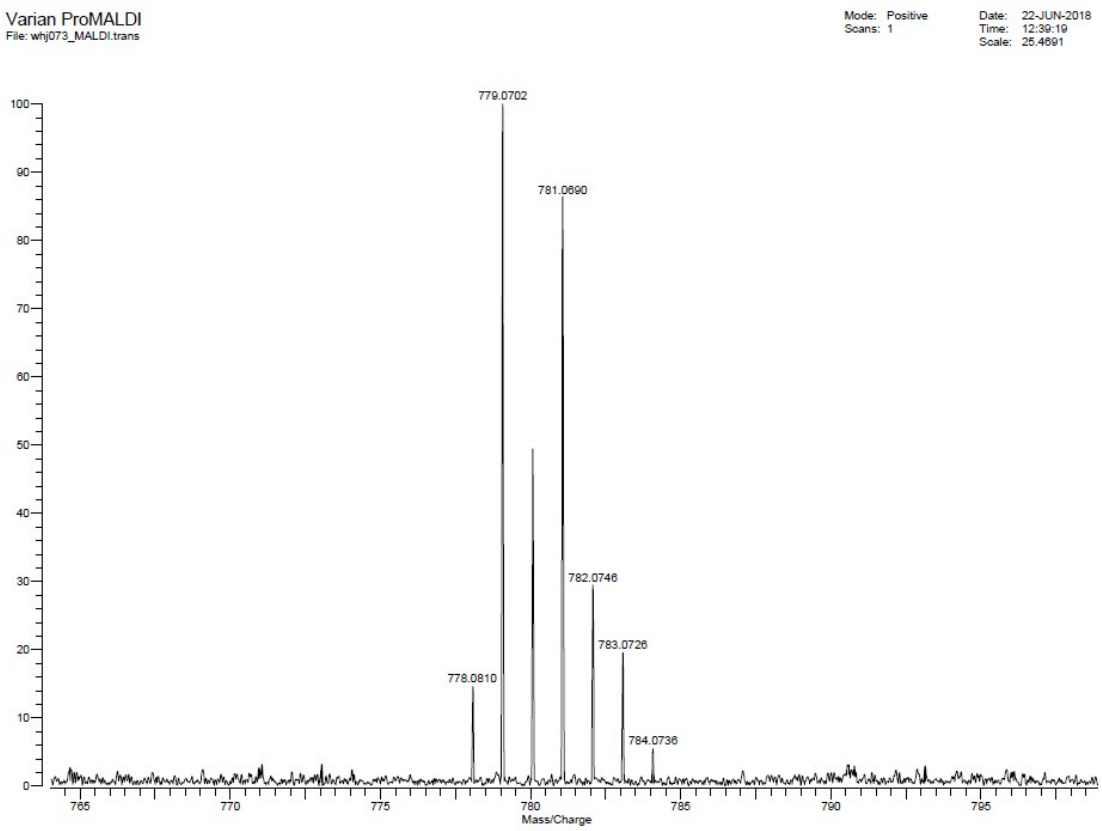

Figure S33. HRMS of **1c**.

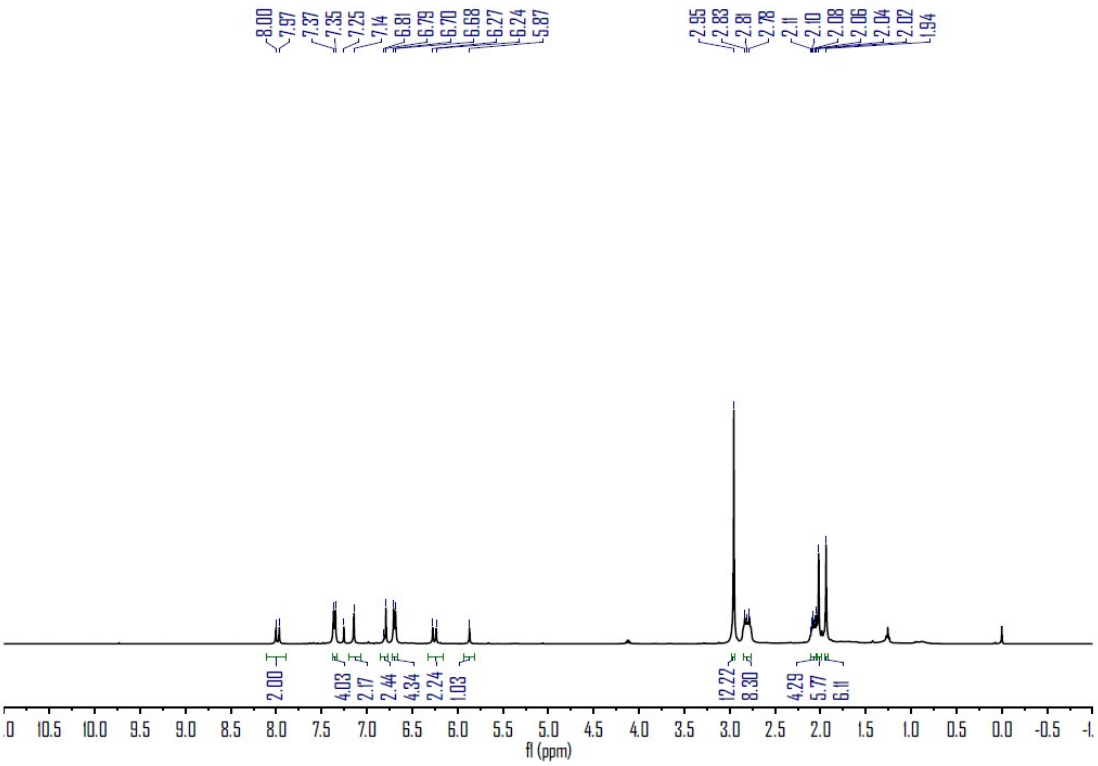

Figure S34. 400 MHz ^{1}H NMR spectrum of **1d** in $CDCl_3$ at room temperature.

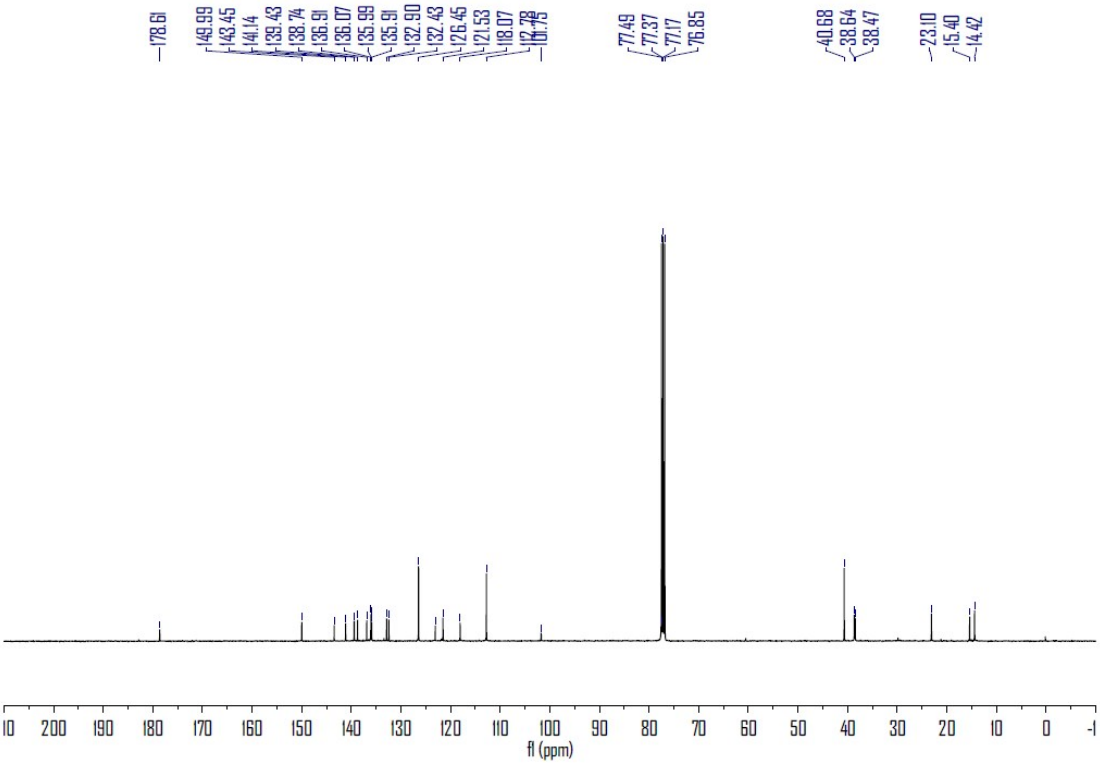

Figure S35. 100 MHz ^{13}C NMR spectrum of **1d** in $CDCl_3$ at room temperature.

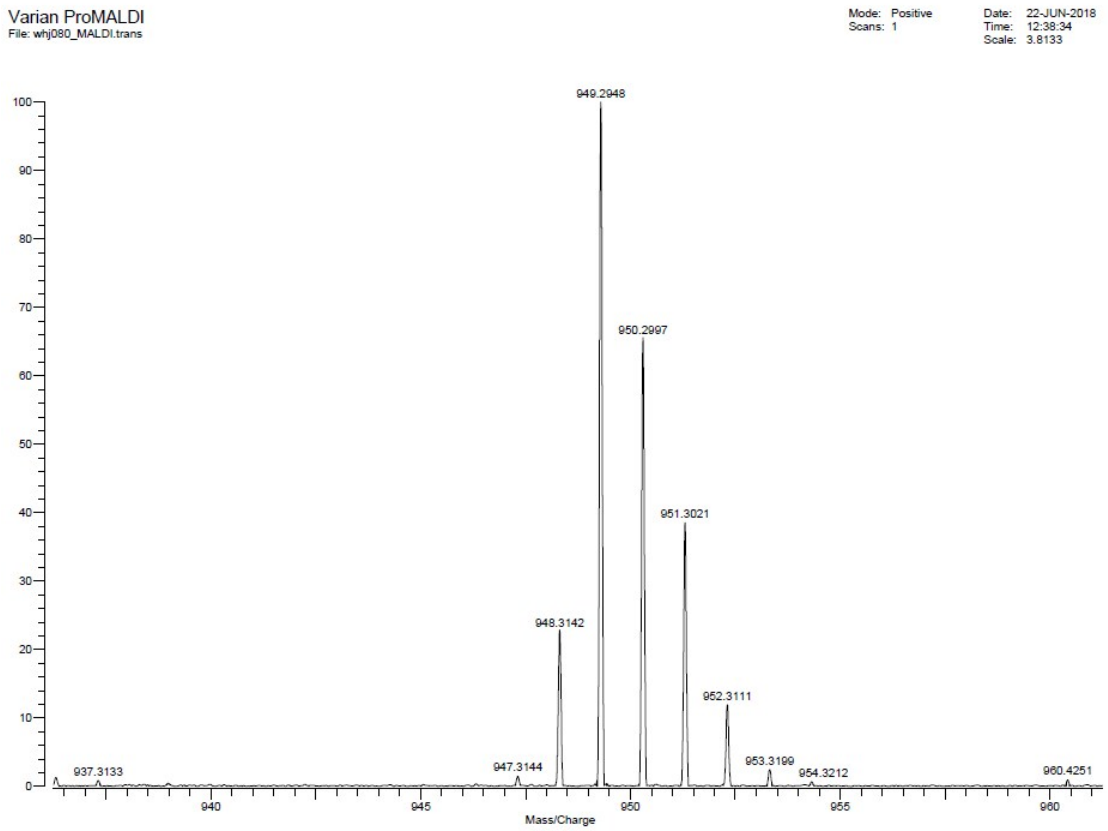

Figure S36. HRMS of **1d**.

8. REFERENCES

1 Q. Zou, J. Jin, B. Xu, L. Ding and H. Tian, *Tetrahedron*, 2011, **67**, 915-921.

2 L. Hou, X. Zhang, T. C. Pijper, W. R. Browne and B. L. Feringa, *J. Am. Chem. Soc.*, 2014, **136**, 910-913.

3 M. Irie, T. Lifka, S. Kobatake and N. Kato, *J. Am. Chem. Soc.*, 2000, **122**, 4871-4876.

4 Gaussian 09, Revision B.01, M. J. Frisch, G. W. Trucks, H. B. Schlegel, G. E. Scuseria, M. A. Robb, J. R. Cheeseman, G. Scalmani, V. Barone, B. Mennucci, G. A. Petersson, H. Nakatsuji, M. Caricato, X. Li, H. P. Hratchian, A. F. Izmaylov, J. Bloino, G. Zheng, J. L. Sonnenberg, M. Hada, M. Ehara, K. Toyota, R. Fukuda, J. Hasegawa, M. Ishida, T. Nakajima, Y. Honda, O. Kitao, H. Nakai, T. Vreven, J. A. Montgomery, Jr., J. E. Peralta, F. Ogliaro, M. Bearpark, J. J. Heyd, E. Brothers, K. N. Kudin, V. N. Staroverov, T. Keith, R. Kobayashi, J. Normand, K. Raghavachari, A. Rendell, J. C. Burant, S. S. Iyengar, J. Tomasi, M. Cossi, N. Rega, J. M.

Millam, M. Klene, J. E. Knox, J. B. Cross, V. Bakken, C. Adamo, J. Jaramillo, R. Gomperts, R. E. Stratmann, O. Yazyev, A. J. Austin, R. Cammi, C. Pomelli, J. W. Ochterski, R. L. Martin, K. Morokuma, V. G. Zakrzewski, G. A. Voth, P. Salvador, J. J. Dannenberg, S. Dapprich, A. D. Daniels, O. Farkas, J. B. Foresman, J. V. Ortiz, J. Cioslowski and D. J. Fox, Gaussian, Inc., Wallingford CT, 2010.

5 A. D. Becke, *J. Chem. Phys.*, 1993, **98**, 5648-5652.

6 R. Ditchfield, W. J and J. A. Hehre, Pople, *J. Chem. Phys.*, 1971, **54**, 724-728.